

# Decipherable Classification of Glaucoma using Deep Neural Network Leveraging XAI

by

Touhidul Islam Chayan

17101362

Anita Islam

17301021

Anika Rahman Tonny

18101569

Eftykhar Rahman

18301041

A thesis submitted to the Department of Computer Science and Engineering  
in partial fulfillment of the requirements for the degree of  
B.Sc. in Computer Science and Engineering

Department of Computer Science and Engineering  
Brac University  
January 2022

## **Declaration**

It is hereby declared that

1. The thesis submitted is my/our own original work while completing degree at Brac University.
2. The thesis does not contain material previously published or written by a third party, except where this is appropriately cited through full and accurate referencing.
3. The thesis does not contain material which has been accepted, or submitted, for any other degree or diploma at a university or other institution.
4. We have acknowledged all main sources of help.

### **Student's Full Name & Signature:**

---

Touhidul Islam Chayan  
17101362

---

Anita Islam  
17301021

---

Anika Rahman Tonny  
18101569

---

Eftykhar Rahman  
18301041

# Approval

The thesis/project titled “Decipherable Classification of Glaucoma using Deep Neural Network Leveraging XAI” submitted by

1. Touhidul Islam Chayan (17101362)
2. Anita Islam (17301021)
3. Anika Rahman Tonny (18101569)
4. Eftykhar Rahman (18301041)

Of Fall, 2021 has been accepted as satisfactory in partial fulfillment of the requirement for the degree of B.Sc. in Computer Science and Engineering on January 18, 2022.

## Examining Committee:

Supervisor:  
(Member)



---

MD Tanzim Reza  
Lecturer  
Computer Science and Engineering  
Brac University

Program Coordinator:  
(Member)

---

Md. Golam Rabiul Alam, PhD  
Associate Professor  
Computer Science and Engineering  
Brac University

Head of Department:  
(Chair)

---

Sadia Hamid Kazi  
Chairperson and Associate Professor  
Department of Computer Science and Engineering  
Brac University

## **Ethics Statement**

We, the members, hereby and genuinely declare that this thesis is based on our thorough study findings. This report appropriately notes and cites all of the materials that were utilized. This research work, in its entirety or in part, has never been submitted to another university or institution for the purpose of awarding a degree or for any other purpose.

# Abstract

Glaucoma is the second driving reason for partial or complete blindness among all the visual deficiencies which mainly occurs because of excessive pressure in the eye due to anxiety or depression which damages the optic nerve and creates complications in vision. In this research, we used the Glaucoma Dataset in our algorithm to predict outcomes related to Glaucoma, suspicious glaucoma, and non-glaucoma. The main goal of the author of this research was to develop an automated deep learning neural network architecture for early detection of Glaucoma disease. For the classification of glaucoma three Black Box models have been used in the paper, such as Fully Connected Neural Network (FCNNs), Support Vector Machine (SVM), and Conventional Neural Network (CNN). This Black Box model has been described through Explainable Artificial Intelligence (XAI) to achieve the ultimate goal of our research. However, to serve our purpose we have used VGG-16, VGG-19, DenseNet121, InceptionV3 and ResNet50 models for our study. To begin, we pre-processed the images and grouped them into three sets: training, testing, and validation. Afterwards, DCNN models have been initialized with the pre-existing models trained on the imangenet dataset. Conclusively, the training and evaluating of all the DCNN has been done. The validation accuracy of our models we got are as follows: InceptionV3 we got 86.4in DenseNet121 we got 86.8% accuracy, in ResNet50 we got 94.7% accuracy, in VGG-19 we got 93.3% accuracy and lastly in VGG-16 we got 88.6% accuracy. As follows, after 50 epochs, RestNet50 got the highest score among the other models with a validation accuracy of 94.7Afterwards we compared all models' accuracy and loss graph together, where we can see that VGG-19 and ResNet50 were the Good-Fit than the other models. As a result, our research achieved outstanding classification accuracy in a short period of time. However, it seems to be vital to understand that a human can rely on black-box level Deep Learning models to make decisions. Throughout this work, a hybrid approach combining image processing with deep learning has been used with the support of XAI to assure reliable glaucoma detection at an early stage

**Keywords:** Glaucoma, Blindness, Diagnosis, Neural Network, XAI, Goal.

## **Acknowledgement**

Firstly, all praise to the Great Allah for whom our thesis have been completed without any major interruption.

Secondly, to our supervisor MD Tanzim Reza sir for his kind support and advice in our work. He helped us whenever we needed help.

And finally to our parents without their throughout support it may not be possible. With their kind support and prayer we are now on the verge of our graduation.

# Table of Contents

<b>Declaration</b>	<b>i</b>
<b>Approval</b>	<b>ii</b>
<b>Ethics Statement</b>	<b>iii</b>
<b>Abstract</b>	<b>iv</b>
<b>Acknowledgment</b>	<b>v</b>
<b>Table of Contents</b>	<b>vi</b>
<b>List of Figures</b>	<b>viii</b>
<b>List of Tables</b>	<b>x</b>
<b>Nomenclature</b>	<b>xi</b>
<b>1 Introduction</b>	<b>1</b>
1.1 Motivation . . . . .	1
1.2 Introduction . . . . .	2
1.3 Research Objectives . . . . .	3
<b>2 Background</b>	<b>4</b>
2.1 Problem Statement . . . . .	4
<b>3 Literature Review</b>	<b>6</b>
3.1 Literature Review . . . . .	6
<b>4 Proposed Model</b>	<b>10</b>
4.1 Proposed Model . . . . .	10
4.2 Work Plan . . . . .	12
<b>5 Implementation</b>	<b>13</b>
5.1 Fundamentals of Deep Learning . . . . .	13
5.2 Dataset, Libraries, and Tools . . . . .	14
5.3 Architecture of the Proposed Model . . . . .	15
5.3.1 VGG-16 . . . . .	16
5.3.2 Inception V3 . . . . .	17
5.3.3 VGG-19 . . . . .	18
5.3.4 ResNet50 . . . . .	19

5.3.5	DenseNet121	20
5.4	Fine Turing	20
5.4.1	Segments of CNN	22
5.4.2	Convolutional Operation	22
5.4.3	Pooling Operation	23
5.4.4	Flattening Layers	24
5.4.5	Fully Connected Layers	25
5.4.6	Batch Normalization	25
5.4.7	Dropout	25
5.5	Analysis	26
5.6	Result	42
<b>6</b>	<b>Conclusion</b>	<b>46</b>
6.1	Conclusion	46
<b>Bibliography</b>		<b>51</b>

# List of Figures

4.1	Blackbox models confirming glaucoma through images . . . . .	10
4.2	Blackbox models decision making explanation through LIME . . . . .	10
4.3	Work plan of the whole project . . . . .	12
5.1	Hidden Layer Between Input and Output Layers . . . . .	13
5.2	Sample Data form LAG-Dataset . . . . .	14
5.3	Sample Data form LAG-Dataset . . . . .	16
5.4	Model Summary of VGG-16 . . . . .	16
5.5	Architecture of VGG-16 . . . . .	17
5.6	The three inception modules . . . . .	17
5.7	Model Summary of InceptionV3 . . . . .	18
5.8	Model Summary of VGG-19 . . . . .	19
5.9	Architecture of VGG-19 . . . . .	19
5.10	Model Summary of ResNet50 . . . . .	20
5.11	Model Summary of DenseNet121 . . . . .	21
5.12	Fine-tuning by keeping the feature extractor's final layers trainable . .	21
5.13	CNN Classifier . . . . .	22
5.14	On the input tensor, a kernel is applied, resulting in a feature map . .	23
5.15	Planes shown are a feature map . . . . .	23
5.16	Pooling Operation . . . . .	23
5.17	Max and Average Pooling . . . . .	24
5.18	Pooling Matrix to Flattening. . . . .	24
5.19	Fully Connected CNN classifying between classes . . . . .	25
5.20	Fully Connected CNN classifying between classes . . . . .	26
5.21	VGG-16 Model Train and Test Accuracy . . . . .	27
5.22	VGG-16 Model Train and Test Loss . . . . .	27
5.23	VGG-19 Model Train and Test Accuracy . . . . .	28
5.24	VGG-19 Model Train and Test Loss . . . . .	28
5.25	ResNet50 Model Train and Test Accuracy . . . . .	29
5.26	ResNet50 Model Train and Test Loss . . . . .	29
5.27	DenseNet121 Model Train and Test Accuracy . . . . .	30
5.28	DenseNet121 Model Train and Test Loss . . . . .	30
5.29	InceptionV3 Model Train and Test Accuracy . . . . .	31
5.30	InceptionV3 Model Train and Test Loss . . . . .	31
5.31	All Model's Train Test Accuracy and Loss Curve . . . . .	32
5.32	True and Predicted Train scores of DenseNet121 . . . . .	33
5.33	True and Predicted Train scores of InceptionV3 . . . . .	33
5.34	True and Predicted Train scores of VGG-16 . . . . .	34

5.35 True and Predicted Train scores of VGG-19 . . . . .	34
5.36 True and Predicted Train scores of ResNet50 . . . . .	35
5.37 Misclassified images for all models with and without preprocessing . . . . .	36
5.38 Misclassified image with preprocessing and Superpixels focused area by Lime in DenseNet121 . . . . .	37
5.39 Lime Explanation for DenseNet121 . . . . .	37
5.40 Misclassified image with preprocessing and Superpixels focused area by Lime in InceptionV3 . . . . .	38
5.41 Lime Explanation for InceptionV3 . . . . .	38
5.42 Misclassified image with preprocessing and Superpixels focused area by Lime in VGG-16 . . . . .	39
5.43 Lime Explanation for VGG-16 . . . . .	39
5.44 Misclassified image with preprocessing and Superpixels focused area by Lime in VGG-19 . . . . .	40
5.45 Lime Explanation for VGG-19 . . . . .	40
5.46 Misclassified image with preprocessing and Superpixels focused area by Lime in ResNet50 . . . . .	41
5.47 Lime Explanation for ResNet50 . . . . .	41
5.48 Lime Explanation for all models single image predictions . . . . .	42
5.49 Single Image Predictions for all Model . . . . .	42
5.50 Batch Predictions for DenseNet121 . . . . .	43
5.51 Batch Predictions for InceptionV3 . . . . .	43
5.52 Batch Predictions for VGG-16 . . . . .	44
5.53 Batch Predictions for VGG-19 . . . . .	44
5.54 Batch Predictions for ResNet50 . . . . .	45

# List of Tables

5.1	Distribution of data with labels . . . . .	14
5.2	Outline of the InceptionV3 architecture . . . . .	18
5.3	True and Predicted Test scores of all Model . . . . .	35
5.4	True and Predicted Test scores of all Model . . . . .	36

# Nomenclature

The next list describes several symbols & abbreviation that will be later used within the body of the document

*AI* Artificial Intelligence

*AMD* Age-related Macular Degeneration

*CADx* Computer-aided diagnostics

*CNN* Convolution Neural Network

*DL* Deep Learning

*FCNN* Fully Connected Neural Network

*LIME* Local Interpretable Model-agnostic Explanations

*OCT* Optical Coherence Tomography

*OCT* Optical Coherence Tomography

*OOP* Object Oriented Programming

*SHAP* SHapley Additive exPlanations

*SVM* Support Vector Machine

*XAI* Explainable AI

# Chapter 1

## Introduction

### 1.1 Motivation

Glaucoma is one of the most painful diseases caused by excessive levels of pressure in the eyes which creates a permanent loss of vision. It is also known as the ‘silent thief of sight’ as it cannot be detected at an early stage [1]. We are going to use Explainable AI (XAI) to classify scanned images of eyes that have glaucoma. XAI proposes the report to the decision of Artificial Intelligence which means Deep Learning or Black Box to the extent that is human interpretable. Deep Learning (DL) is a subset of Artificial Intelligence (AI) dependent on profound neural networks which have made striking leaps forwards in clinical imaging, especially for image characterization and pattern acknowledgment [2]. The use of Deep Learning (DL) is increasing in glaucoma research because these models can accomplish high precision, issues with trust, interpretability, and experimental utility structure hindrances to occurring clinical practice. The main purpose of this study is to represent whether and how deep learning-based measurements can be utilized for glaucoma execution in the clinic [3].

In our glaucoma dataset, we have some features for suspicious glaucoma and non-suspicious glaucoma. However, data visualization methods aim to produce more transparent and explainable decisions. In addition, CNN Based models are visually explainable for decision making and have gained significant attention in image classification [4]. A few works focus on preparing a Convolution Neural Network (CNN) by brute force while others use division and element extraction methods to identify glaucoma [5]. To apply for XAI we took Conventional Neural Network (CNN), Support Vector Machine (SVM), and Fully Connected Neural Network (FCNN). XAI frameworks such as LIME, SHAP, ELI5, AIX360, Skater are used for building trust among humans about the decisions made by AI models which are possibly making the black box models more transparent. Moreover, working with these AI models is not understandable by the common man and professionals. Additionally, AI and Machine Learning are essential for building trust among humans for decision making which is only possible by making black-box models more transparent through Explainable AI Frameworks which tries to explain their working.

## 1.2 Introduction

Glaucoma is a gathering of eye illnesses wherein the optic nerve is harmed prompting irreversible loss of vision. By and large, this is because of an expanded pressing factor inside the eye. The eye creates a liquid called fluid humor which is emitted by the ciliary body into the back chamber - a space between the iris and the focal point. It at that point courses through the apprentice into the foremost chamber between the iris and the cornea. From here, it channels through a wipe-like design situated at the foundation of the iris considered the trabecular meshwork, and leaves the eye. In a solid eye, the pace of discharge adjusts the pace of seepage. In individuals with glaucoma, the seepage waterway is part of the way or totally hindered. Liquid develops in the chambers and this expands pressure inside the eye. The pressing factor drives the focal point back and pushes on the glassy body which thus packs and harms the veins and nerve strands running at the rear of the eye. These harms bring about patches of vision misfortune, and whenever left untreated, may prompt absolute visual impairment. There are two significant kinds of glaucoma: open-angle and angle-closure.

Open-angle glaucoma, or chronic glaucoma, is brought about by an incomplete blockage of the waste trench. The point between the cornea and the iris is "open", which means the passageway to the waterway is clear, however, the progression of watery humor is more slow than typical. The pressing factor develops continuously in the eye throughout a significant period. Side effects show up continuously, beginning from fringe vision misfortune, and may go on unseen until focal vision is influenced. Movement of glaucoma can be halted with medicines, however, part of the vision that is now lost can't be reestablished. This is the reason it's vital to distinguish early indications of glaucoma with standard eye tests.

Angle-closure glaucoma, or acute glaucoma, is brought about by an abrupt and complete blockage of fluid humor waste. The pressing factor inside the eye rises quickly and may prompt absolute visual deficiency rapidly. Certain anatomical highlights of the eye, for example, limited seepage point, shallow foremost chamber, slender and saggy iris, make it simpler to foster intense glaucoma. Commonly, this happens when the understudy is expanded and the focal point has adhered to the rear of the iris. This squares the fluid humor from coursing through the understudy into the foremost chamber. Collection of liquid in the back chamber pushes on the iris, making it swell outward and square the waste point. Acute angle-closure glaucoma is a visual crisis and requires quick consideration.

However, it's one of the leading causes of blindness for people over the age of 60. Statistics show that even with the treatment 15% to 20% of patients become blind. For this reason, in this research, we are going to apply Explainable AI to detect Glaucoma in a better way than exists. As the diagnosis of glaucoma is a complicated and expensive process, the application of a Deep Neural network leveraging XAI can give more improvement in understanding or detecting many problems related to glaucoma disease.

## 1.3 Research Objectives

The field of Explainable Artificial Intelligence has filled dramatically lately with innovations, techniques, and applications arising at a fast rate. A considerable lot of these progressions have been utilized to improve the conclusion and the executives of glaucoma. We intend to give an outline of ongoing distributions in regards to the utilization of man-made consciousness to improve the recognition and treatment of glaucoma.

According to modern medical science, glaucoma is diagnosed in four different ways. Initially, glaucoma is diagnosed by machine where the pressure is measured inside the eye. Here the whole diagnostic test is called Tonometry and the intraocular pressure is measured throughout this process. Apart from this, there is a prerequisite of this test which is a visual feel test. In this test, the patient is asked to close one eye and the doctor moves his hand from top to bottom, bottom to top, left to right, and right to left. In this way, the doctor checks the patient's visibility through one eye. Moreover, there is another way of diagnosing glaucoma which is the Imaging Test where the main motive is to check the depth of eyes by showing pictures. However, the final diagnosis is pachymetry where pachymetry is a medical device that is used to measure the thickness of the eye's cornea. In the above ways, glaucoma can be diagnosed and partial or complete blindness could be prevented.

AI classifiers and deep learning algorithms have been created to self-sufficiently recognize early primary and useful changes of glaucoma utilizing diverse imaging and testing modalities like fundus photography, optical cognizance tomography, and standard computerized perimetry. Artificial Intelligence has additionally been utilized to further portray structure-work connection in glaucoma. Additionally, "structure-structure" predictions have been effectively assessed. Other AI strategies using complex measurable demonstrating have been utilized to distinguish glaucoma movement, just as to foresee future movement. Though not yet endorsed for clinical use, these artificial intelligence methods can essentially improve glaucoma analysis and the board.

# Chapter 2

## Background

### 2.1 Problem Statement

Glaucoma is a very common group of eye diseases caused by damage to the optic nerve that connects the eye to the brain and if untreated, it causes permanent loss of vision. It is the second most popular cause of blindness globally. As per experiments, it is tracked down that the conclusion of the experts or ophthalmologists is abstract. This may cause a few misinterpretations when the glaucoma is distinguished as inaccurate, for example, false-positive and false-negative cases. Likewise, glaucoma is asymptomatic in the beginning phase. The harm advances gradually and it has no manifestations or early admonition signs until the vision is lost in the later stage. Additionally, if it tends to be distinguished in the beginning, the visual sight will be saved. It is shown that treatment and standard tests can forestall vision misfortune in individuals just at a beginning phase. On the other hand, if the vision loss has already occurred, the treatment can delay or hinder further vision loss [6].

There are mainly two types of glaucoma. Primary glaucoma also called chronic glaucoma is caused by prolonged intraocular pressure in the eye whereas secondary glaucoma is caused by sudden events such as an injury to the eye or inflammation in the eye or the use of steroids. Both primary and secondary glaucoma can be further classified as open-angle glaucoma and closed-angle glaucoma. Open-angle glaucoma is the most common form of glaucoma and is responsible for 90% of the cases [7]. In open-angle glaucoma, there is a wide and open angle between the cornea and iris. But in the case of closed-angle glaucoma, the angle is much narrower. Each of these subdivisions can be further divided into classes depending on conditions such as acute, intermittent, chronic, post status, etc. And there are other minor variants of glaucoma such as pigmentary glaucoma, exfoliation glaucoma, primary juvenile glaucoma, etc. In traditional cases, Ophthalmologists use Optical Coherence Tomography or OCT for detecting Glaucoma. Optical Coherence Tomography or OCT is generally utilized for clinical imaging methods. OCT is an optical sign procurement and preparation strategy that catches optic pictures in a three-dimensional picture. Both OCT and ophthalmologists are having a similar issue which is lacking and costly. They must be found in enormous emergency clinics or private emergency clinics. Some glaucoma patients are deficient assets. This can make patients seek a late glaucoma treatment and be awful for their eye wellbeing. The requirement for specialists and a lot of costs are constraints of potential in mass evaluating for early

discovery. To take care of the issue of OCT pictures, fundus im-ages are chosen to be input pictures for this venture. A fundus camera is one more sort of camera that can be utilized to catch retina pictures. Fun-does camera has more affordable costs contrasting and OCT pictures. It very well may be found in each region's clinical focus, not just enormous clinics like OCT. Fundus pictures can be utilized for glaucoma finding through the CDR strategy [8].

Since glaucoma is such a prominent reason for blindness around the world, we must apply our knowledge of classification techniques to classify the various types of glaucoma for the betterment of the world. However, we are portraying and evaluating Convolutional Neural Organization (CNN) models for the discovery of glaucoma dependent on Optical Coherence Tomography (OCT) Retinal Nerve Fiber Layer (RNFL) likelihood maps. Such CNN models can work in pairs with human specialists to keep up with large eye health and assist recognition of visual deficiency causing eye sickness []. We can easily use binary classifiers to differentiate between images of primary glaucoma and secondary glaucoma and then we can use another binary classifier to differentiate between images of open-angle glaucoma and closed-angle glaucoma. In this study, we are going to use Explainable AI (XAI) to classify scanned images of eyes that have glaucoma.

# Chapter 3

## Literature Review

### 3.1 Literature Review

Glaucoma is one of the most common causes of permanent blindness around the world, from the article [10]. As when the pressure inside the eye is too high in a particular nerve that moment glaucoma will develop and it will also create eye ache. The working mechanisms of the different diagnosis tools like tonometers, gonioscopy, scanning laser tomography, etc are available for the treatment and detection but there are some advantages and disadvantages which sometimes create boundaries. For this, there should be an evaluation of how this works. But with using deep learning the boundaries can be removed. As the XAI concept can be understood by humans which will be closer to the human brain to understand.

Recent breakthroughs in machine learning (ML) have the potential to significantly enhance retinal disease screening and diagnostic accuracy according to [11]. The recent most demanding field of explainable artificial intelligence (XAI) attempts to focus on Glaucoma disease. As a result, the necessity for expert-level review in assessing their efficacy becomes unavoidable. In a series of tests, we illustrate the efficacy of our method. XAI is vastly classified in these categories- Application-Grounded Evaluation, Human-Grounded Evaluation, and Functionally Grounded Evaluation. Some of the findings from this paper are as follows: (i) Recent breakthroughs in machine learning promise to significantly enhance retinal disease screening and diagnostic accuracy. Multiple eye illnesses, including diabetic retinopathy, age-related macular degeneration (AMD), glaucoma, and other anomalies associated with retinal diseases, to keep track of their progress. This has been diagnosed with expert-level accuracy using systems built using these methodologies. (ii) XAI's purpose is to decode the decision of Artificial Intelligence which means Deep Learning or Machine learning black box to the extent that it is human-interpretable. (iii) Used two of the most current visual explanation methods to assess the visual explanation on the provided dataset which are SIDU and GRAD-CAM. As a result, in addition to enhancing the tool's accuracy, the concept of trust, as well as the requirement for openness and robustness, emphasizes the need of investigating the impact of expert review in the context of XAI approaches.

Computer-aided diagnostics(CADx) tools are still struggling to detect glaucoma eye illness according to author Qaisar Abbas [12]. Glaucoma is the main reason for

visual disability in the whole world. His writings revealed that the Softmax linear classifier makes the ultimate judgment to distinguish between glaucoma and non-glaucoma retinal fundus images. Glaucoma-Deep, the suggested method, was evaluated on 1200 retinal pictures gathered from publicly and privately available datasets. Then the sensitivity (SE), specificity (SP), accuracy (ACC), and precision (PRC) statistical measurements were used to evaluate the performance of the Glaucoma-Deep system. In general, the SE of 84.50%, SP of 98.01%, ACC of 99%, and PRC of 84% values were achieved through this. When compared to other systems, the Nodular-Deep approach produced much better outcomes. As a result, the Glaucoma-Deep system can quickly identify glaucoma eye illness, solving the problem of clinical specialists during large-scale eye-screening processes.

Glaucoma is the leading cause of blindness in the world, and there is no treatment [13]. If it is not diagnosed at an early stage, it can surely lead to irreversible blindness. If vision loss is detected early enough, there are treatments available to prevent it. Because it is a significant chronic eye condition that leads to irreversible blindness. Glaucoma has been on the rise in recent years. Faults in the nerve fiber layer of the retina are diagnosed before apparent abnormalities at the head of the optic nerve and defects in the visual field when 40 percent of axons have been irreversibly destroyed. According to the World Health Organization (WHO) and the World Association of Glaucomatologists (WGO), 66.8 million individuals worldwide suffered from glaucoma in 2010, with 6.7 million becoming blind as a result of the disease.

Another version of the deep-learning (DL) algorithm was developed in [6] to detect glaucoma disease through extracting several parameters such as 52 total deviation, mean deviation, and pattern standard deviation values. Here the writer used a Deep learning classifier such as a deep feed-forward neural network (FNN). The authors, on the other hand, integrated their DL classifier with older machine learning classifiers including random forests (RF), gradient boosting, support vector machine, and neural network (NN). As a result, the authors provided a deep ensemble solution for glaucoma illness detection. A deep FNN classifier was used to get 92.5 percent of the AUC value, according to the authors.

We learned The impact of artificial intelligence in the diagnosis and management of glaucoma from [15]. Computerized automated visual field testing represents a significant improvement in mapping the island of vision, allowing visual field testing to become a cornerstone in diagnosing and managing glaucoma. Goldbaum developed a two-layer neural network for analyzing visual fields in 1994 et al.[8] . This network classified normal and glaucomatous eyes with the same sensitivity (65% ) and specificity (72% ) as two glaucoma specialists.

According to the writer [16] To diagnose illnesses, different healthcare systems employ content-based picture analysis and computer vision algorithms. Fundus pictures recorded with a fundus camera are used to identify abnormalities in the human eye. Glaucoma is the second most common cause of neurodegenerative sickness among eye illnesses. Glaucoma has no symptoms in its early stages, and if the condition is not treated, it can result in total blindness. Glaucoma can be detected early

enough to prevent irreversible visual loss. Although manual inspection of the human eye is a viable option, it is reliant on human effort. The goal of this review article is to provide a complete overview of the numerous varieties of glaucoma, their causes, prospective treatments, publicly accessible image benchmarks, performance measures, and different methodologies based on digital image processing, computer vision, and deep learning. The review paper examines a variety of published research models for detecting glaucoma, ranging from low-level feature extraction to contemporary deep learning developments. The advantages and disadvantages of each strategy are examined in-depth, and the findings of each category are summarized using tabular representations.

As previous data shows how glaucoma disease gradually leads to blindness[8]. If we can detect glaucoma early it can be preventable against developing more serious conditions, they claimed. Cup-to-disc Ratio or CDR is an essential clinical indicator for glaucoma diagnosis in their research. Their objective is to develop a system that can provide a proper path to compute CDR results with the highest possible accuracy. They used 44 retinal images from Mettapracharak hospital to evaluate the performance, of which 29 retinal images were patients with no glaucoma and 15 were with glaucoma disease. Which shows impressive accuracy. Then compare the value of CDR which is more than 0.65 is used to access a patient as a possible glaucoma case. CDR value between clinical result and edge detection with power raw transformation approach. Where the proposed method was 5.14%. The percentage error by using their proposed method for optic disc segmentation, optic cup segmentation and CDR are 2.49%, 5.8%, and 5.14%, respectively. The CDR is a crucial clinical sign for determining a person's risk of developing glaucoma. For this, in their paper, they presented a method to calculate the CDR automatically from fundus images the author added.

Following the enormous success of one class of mathematical models, the artificial neural network, artificial intelligence, or AI has risen. Deep learning, a recently invented method, has taken over current scientific discourse, penetrating areas such as physics, chemistry, engineering, biology, and medicine [17]. This leads to a discussion on current solutions and state-of-the-art, with some drawbacks that may limit clinical adoption. Glaucoma is usually linked with increased intraocular pressure (IOP), which affects the overall visual field of the eye over time[18][19]. Research on glaucoma suggests that the disease's development is influenced by several interconnected bodily mechanisms. There are two kinds of glaucoma: open-angle and closed-angle. The angle refers to the length of contact between the iris and the cornea; if the length is long, the related illness is called open-angle glaucoma; if the length is short, it is called closed-angle glaucoma, they added [19]. Not only can glaucoma affect the patient's eyesight, but it's also linked to a hearing disability (Greco et al. in The American Journal of Medicine, 2016) [19]. They reviewed the complete techniques of glaucoma detection using Deep neural networks.

The pathogenesis of glaucoma appears to be dependent on several interconnected pathogenetic mechanisms, including mechanical effects characterized by excessive intraocular pressure, reduced neutrophil produce, hypoxia, excitotoxicity, oxidative stress, and the involvement of autoimmune processes, according to new evidence

[19]. Hearing loss has also been linked to the development of glaucoma. In normal-tension glaucoma patients with hearing loss, antiphosphatidylserine antibodies of the immunoglobulin G class were shown to be more prevalent than in normal-tension glaucoma patients with normacusis. The World Health Organization reports that glaucoma affects approximately 60 million people worldwide. By the year 2020, it is expected that approximately 80 million people will suffer from glaucoma, which is anticipated to result in 11.2 million cases of bilateral blindness [20]. This is why it needs to be treated as early as possible according to the authors.

The visual fields from an automated perimeter were taught to be interpreted by neural networks. The scientists tested the trained neural networks' capacity to distinguish between normal and glaucoma-affected eyes [21]. After research, we got that, Glaucoma specialists and a trained two-layered network both got around 67 percent of the answers right. The two glaucoma experts had a sensitivity of 59 percent, while the two-layered network had a sensitivity of 65 percent. For the specialists and the two-layered network, the corresponding specificities were 74% and 71%, respectively. About 74 percent of the time, the experts and the network agreed, indicating that there was no substantial discrepancy between the testing methodologies. The most relevant visual field locations were discovered using feature analysis and a one-layered network. Here the authors conclude that a neural network may be taught to evaluate visual fields for glaucoma as well as a professional reader. The researchers compared the backpropagation learning approach used by automated neural networks to the methods employed by two glaucoma specialists to identify the center's 24 degrees automated perimetry visual fields from 60 normal and 60 glaucomatous eyes. However The neural network like deep learning has many limitations like a vast number of pictures must be incorporated in DL algorithms for them to predict with high sensitivity and specificity, moreover obtaining and storing a large number of photos comes with time limits and technological challenges. Furthermore, for such databases to remain current and prevent system-wide algorithm failure, they may need to be updated regularly. And most importantly Because the mechanism of DL's prediction is unclear, it is referred to as a "black box", which clearly shows its limitations. To resolve these issues using the XAI can be a big step towards Glaucoma detection.

# Chapter 4

## Proposed Model

### 4.1 Proposed Model

We will use Deep Learning in our work which is a BlackBox function. Generally, Black boxes work excellently but their structure won't give you any insights that will explain how the function is being approximated. For this, we will use LIME which is one of the most popular XAI-based python libraries. There are a lot of XAI frameworks that explain the BlackBox model's insights by features. XAI functions work well in terms of explaining complex classification models. In short, these functions generate an explanation through charts of graphs for a complex model's prediction which are also pretty fast. In Figure 4.1 we will see how black boxes work.

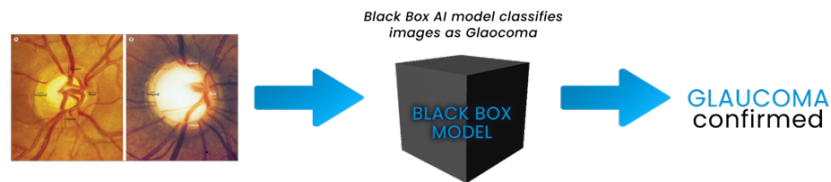


Figure 4.1: Blackbox models confirming glaucoma through images

In Figure 4.2 we will see how black boxes actually work with the help of lime.

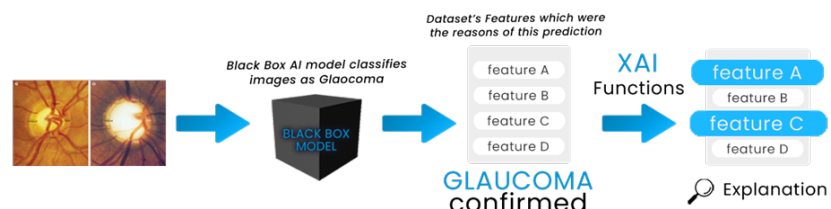


Figure 4.2: Blackbox models decision making explanation through LIME

Here we can see BlackBox models generate a result or output based on some features from the given/training datasets. And through lime, we can have a visualization from which features the output was based on.

In our Glaucoma dataset, we have some features for Suspicious glaucoma and Non-glaucoma. In both sections, we have **attention map**, **images**, and **labels** as **1** as the confirmed glaucoma case and **0** as the Non-glaucoma case. To apply XAI, we took **Convolutional Neural Network (CNN)**, **Support Vector Machine (SVM)**, **Fully Connected Neural Network (FCNNs)** as a black box AI model to predict glaucoma with the help of the data. To compile all of these classifications and determine the average of these scores to one single output, we will use the Softmax function. Below a short rendition is being given for the above Deep Learning models.

1. **Convolutional Neural Network (CNN)**: In deep learning, a convolutional neural network (CNN, or ConvNet) is a class of deep neural networks, most commonly applied to analyze visual imagery. We will classify the image data through this model.
2. **Support Vector Machine (SVM)**: SVM is a supervised machine learning classifier that may be used to categorize or to regression problems. It uses a method called the kernel trick to transform your data and then calculates an appropriate boundary between various outputs based on these modifications. With this model, we will get a predicted output.
3. **Fully Connected Neural Network (FCNNs)**: Fully connected neural networks (FCNNs) are a type of artificial neural network where the architecture is such that all the nodes, or neurons, are in one layer, are connected to the neurons in the next layer [22]. This model will also help us to predict and output.
4. **Softmax**: Softmax is a mathematical function that transforms a vector of integers into a vector of probabilities, with the probability of each value proportional to the vector's relative scale. The softmax function is most commonly used as an activation function in a neural network model in applied machine learning. The network is set up to produce N values, one for each classification task class, and the softmax function is used to normalize the outputs, turning them from weighted sum values to probabilities that total to one. Each value in the output of the softmax function is interpreted as the probability of membership for each class. This will compile the outputs of SVM and FCNNs into a single output.

## 4.2 Work Plan

According to our Dataset, we will divide the data in a ratio of 8:2 chronologically training and testing data to classify glaucoma with the help above deep learning models. And through any XAI function, we will explain these black boxes.

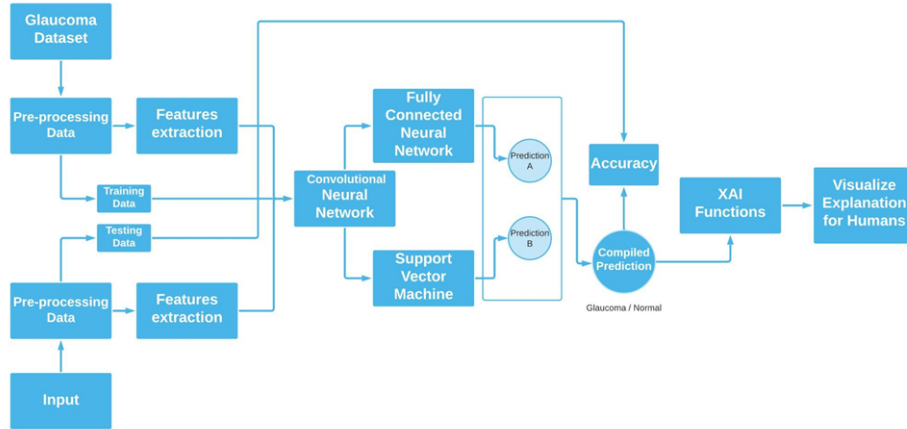


Figure 4.3: Work plan of the whole project

Here in [Figure 4.3], we have shown the whole process from dataset preprocessing to compiled output through Softmax. And with XAI functions, we will explain the black boxes through visualization charts of the used core features which were the main reasons behind the prediction.

# Chapter 5

## Implementation

### 5.1 Fundamentals of Deep Learning

Deep learning is a type of machine learning and artificial intelligence (AI) that imitates the way humans gain certain types of knowledge. While traditional machine learning algorithms are linear, deep learning algorithms are stacked in a hierarchy of increasing complexity and abstraction [23].

Neural Networks are basically made-up of several units which work mimicking the human brain's neurons. Each neuron is connected to another one in order to generate a particular problem to solve. These neurons in AI are called units.

The input layer is the very first neuron of an Artificial brain. It takes raw data from the dataset and passes it to the next-level neurons. And the layer which produces the final output is called the output layer. These input and output layers may contain N number of units. Output layers units may depend on the output layer classes. In between these two layers, there can be N numbers of hidden layers, each containing its own weights and biases so that it can calculate its next neuron's journey. The given weight of the connection is multiplied to its corresponding input and then added up resulting in a weighted sum, on which the activation function implies and produces the activation for that neuron, which is indeed the output of the neuron denoted by  $y$ . Then, an activation function will get triggered as an output for this  $y$ .

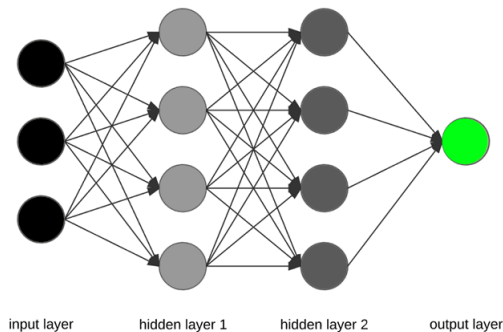


Figure 5.1: Hidden Layer Between Input and Output Layers

## 5.2 Dataset, Libraries, and Tools

As our data are mostly direct fundus images from LAG-Dataset[24]. CNN is being used in this thesis for image classification, as it is a type of model which processes data such as images. Also, it automatically understands low-to high-level patterns of image classification. which helps us to extract higher representations for the image content.



Figure 5.2: Sample Data form LAG-Dataset

This dataset contains 4250 images for **training**, 302 images for testing and 302 images for **validation**. All of these folders have two folders for glaucoma and non-glaucoma. The label for “glaucoma” is 1 and for “non-glaucoma” is 0.

Class	Label	Fundus images	Attention maps
Suspicious Glaucoma	1	1711	1711
Non Glaucoma	0	3143	3143

Table 5.1: Distribution of data with labels

In this study, we are going to use the **python** programming language. It is a high level OOP programming language that has a lot of amazing Machine learning libraries.

For this research we are using :

- IDE (Google Colab Jupyter Notebook)
- GPU (GTX 1660 super OC)

Some of the Libraries that we are going to use are :

**TensorFlow:** TensorFlow is an end-to-end open-source platform for machine learning. It has a comprehensive, flexible ecosystem of tools, libraries, and communities [17].

**Keras:** Keras is the high-level API of TensorFlow 2: an approachable, highly-productive interface for solving machine learning problems [18]

**Matplotlib:** Matplotlib is a comprehensive library for creating static, animated, and interactive visualizations in Python.[25]

**Pandas:** Pandas is an open-source, BSD-licensed library providing high-performance, easy-to-use data structures, and data analysis tools for Python programming [26]

**Numpy:** NumPy offers comprehensive mathematical functions, random number generators, linear algebra routines, Fourier transforms, and more [19]

**Scikit-Learning:** Simple and efficient tools for predictive data analysis · Accessible to everybody, and reusable in various contexts · Built on NumPy, SciPy, and matplotlib [27]

### 5.3 Architecture of the Proposed Model

In deep learning, a convolutional neural network (CNN, or ConvNet) is a class of artificial neural networks, most commonly applied to analyze visual imagery[20].

In this study, a Transfer Learning approach is proposed. The data set's size and features provide a perfect environment for implementing a transfer learning approach, allowing a pre-trained CNN with all of its weights to be utilized to develop a new transfer learning model specialized to identifying Glaucoma with a high degree of accuracy.

We are going with the Fine-Tuning approach of Transfer Learning.

The CNN Models we are using are:

- VGG-16
- InceptionV3
- VGG-19
- ResNet50
- DenseNet121

# Transfer Learning

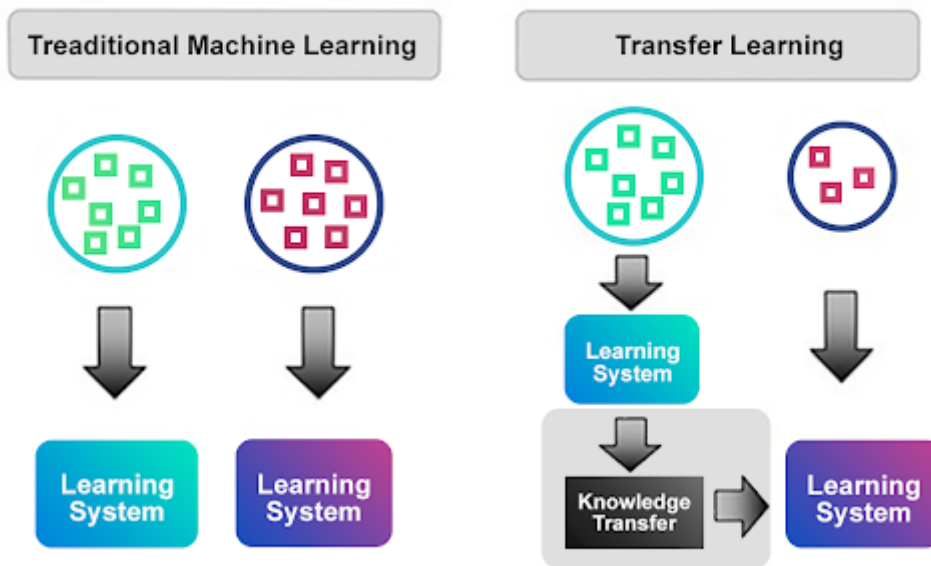


Figure 5.3: Sample Data from LAG-Dataset

### 5.3.1 VGG-16

With 16-19 layers of weights and small convolution filters of (33), the VGG[29] Convolutional Neural Network built by Visual Geometry Group, the University of Oxford has achieved amazing results. ReLU non-linearly is used here for hidden layers.

Here, we used the Keras implementation of the VGG16 model. We used the weights learned from the ImageNet dataset. We didn't use the 3 fully connected layers at the top of the network. Input shape of the images is 224 x 224 and there are 3 channels. First, we flattened the model outputs. We used the "ReLU" activation function for the layers. For predictions, we used the "Softmax" activation function.

In figure 5.4 we can visualize the architecture of the VGG-16 model.

block5_conv2 (Conv2D)	(None, 14, 14, 512)	2359808
block5_conv3 (Conv2D)	(None, 14, 14, 512)	2359808
block5_pool (MaxPooling2D)	(None, 7, 7, 512)	0
flatten (Flatten)	(None, 25088)	0
fc1 (Dense)	(None, 4096)	102764544
fc2 (Dense)	(None, 4096)	16781312
dense (Dense)	(None, 4552)	18649544
=====		
Total params: 152,910,088		
Trainable params: 18,649,544		
Non-trainable params: 134,260,544		

Figure 5.4: Model Summary of VGG-16

In figure 5.5 we can visualize the architecture of the VGG-16 model.

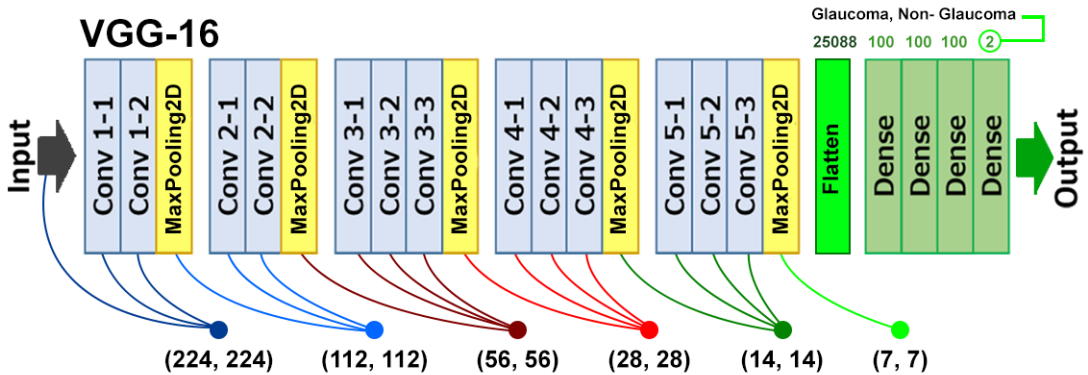


Figure 5.5: Architecture of VGG-16

### 5.3.2 Inception V3

The Inception [30] architecture is made up of several inception modules stacked on top of each other to form a deep neural network, where the inception modules provide the ability to operate them all in parallel and concatenate their outputs into a single output vector for input to the module afterward.

Here we used Keras implementation of inceptionV3 model. We used the weights learned from the ImageNet dataset. We didn't use the 3 fully connected layers at the top of the network. Input shape of the images is 224 x 224 and there are 3 channels. First, we flattened the model outputs. We used the "ReLU" activation function for the layers. For predictions, we used the "Softmax" activation function.

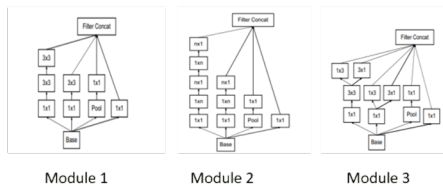


Figure 5.6: The three inception modules

In our proposed transfer learning model, we use InceptionV3, a new form of the inception architecture. Table 5.2 depicts the InceptionV3 network architecture. Each module's output size is the next module's input size.

In figure 5.7 we can visualize our model summary of InceptionV3.

Type	patch size	input size
conv	3 x 3/2	224 x 224 x 3
conv	3 x 3/1	149 x 149 x 32
conv padded	3x3 / 1	147 x 147 x 32
pool	3x3/2	147 x 147 x 64
conv	3×3/1	73 × 73 × 64
conv	3×3/2	71 × 71 × 80
conv	3×3/1	35 × 35 × 192
3×Inception	module 1	35 × 35 × 288
5×Inception	module 2	17 × 17 × 768
2×Inception	module 3	8 × 8 × 1280
pool	8×8	8 × 8 × 2048
linear	logits	1 × 1 × 2048
softmax	classifier	1 × 1 × 1000

Table 5.2: Outline of the InceptionV3 architecture

<code>flatten_14 (Flatten)</code>	<code>(None, 51200)</code>	<code>0</code>	<code>mixed10[0][0]</code>
<code>dense_56 (Dense)</code>	<code>(None, 100)</code>	<code>5120100</code>	<code>flatten_14[0][0]</code>
<code>dense_57 (Dense)</code>	<code>(None, 100)</code>	<code>10100</code>	<code>dense_56[0][0]</code>
<code>dense_58 (Dense)</code>	<code>(None, 100)</code>	<code>10100</code>	<code>dense_57[0][0]</code>
<code>dense_59 (Dense)</code>	<code>(None, 2)</code>	<code>202</code>	<code>dense_58[0][0]</code>
<hr/>			
Total params: 26,943,286			
Trainable params: 5,140,502			
Non-trainable params: 21,802,784			
<hr/>			

Figure 5.7: Model Summary of InceptionV3

### 5.3.3 VGG-19

VGG19 is a variant of the VGG model which in short consists of 19 layers (16 convolution layers, 3 fully connected layers, 5 MaxPool layers, and 1 SoftMax layer). [32] VGG19 has 19.6 billion Flops.

Here, we used the Keras implementation of the VGG19 model. We used the weights learned from the ImageNet dataset. We didn't use the 3 fully connected layers at the top of the network. Input shape of the images is 224 x 224 and there are 3 channels. First, we flattened the model outputs. Then we performed batch normalization. We used a dropout rate of 0.5. We used the “ReLU” activation function for the layers.

For predictions, we used the “Softmax” activation function. For the Gradient Descent, we used the Adam optimizer with a learning rate of  $10^{-5}$ . In Figure 5.8, Our model summary for VGG-19 is given.

block5_conv4 (Conv2D)	(None, 14, 14, 512)	2359808
block5_pool (MaxPooling2D)	(None, 7, 7, 512)	0
flatten_1 (Flatten)	(None, 25088)	0
dense_4 (Dense)	(None, 100)	2508900
dense_5 (Dense)	(None, 100)	10100
dense_6 (Dense)	(None, 100)	10100
dense_7 (Dense)	(None, 2)	202
<hr/>		
Total params: 22,553,686		
Trainable params: 2,529,302		
Non-trainable params: 20,024,384		

Figure 5.8: Model Summary of VGG-19

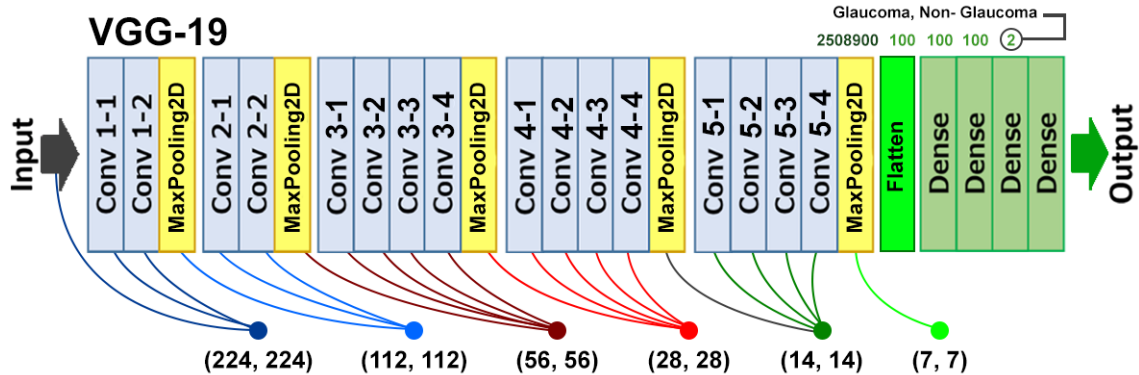


Figure 5.9: Architecture of VGG-19

### 5.3.4 ResNet50

ResNet50 is a version of the ResNet model which has 48 convolution layers and 1 MaxPool layer and 1 average pool layer. Moreover, it has  $3.8 \times 10^9$  floating-point operations. ResNet50 plays an important role in the computer vision and deep learning world. It is mainly used for image recognition and is most commonly applied for analyzing visual imagery. Also, it is a pre-trained Deep Learning model for image classification of the Convolutional Neural Network (CNN). ResNet50 is mainly trained on a million images of 1000 categories from the ImageNet database and there are over 23 million trained parameters which will make it more suitable for image recognition. ResNet50 is deeper than any other network using residual connections.

Here, we used the Keras implementation of the ResNet50 Model. We used the weights learned from the ImageNet dataset. We didn't use the 3 fully connected

layers at the top of the network. Input shape of the images is 224 x 224 and there are 3 channels. First, we flattened the model outputs. Then we performed batch normalization. We used a dropout rate of 0.5. We used the “ReLU” activation function for the layers. Again we performed batch normalization and used a dropout rate of 0.5. For predictions, we used the “Softmax” activation function.

<code>conv5_block3_out (Activation)</code>	<code>(None, 7, 7, 2048)</code>	0	<code>conv5_block3_add[0][0]</code>
<code>flatten (Flatten)</code>	<code>(None, 100352)</code>	0	<code>conv5_block3_out[0][0]</code>
<code>dense (Dense)</code>	<code>(None, 100)</code>	10035300	<code>flatten[0][0]</code>
<code>dense_1 (Dense)</code>	<code>(None, 100)</code>	10100	<code>dense[0][0]</code>
<code>dense_2 (Dense)</code>	<code>(None, 100)</code>	10100	<code>dense_1[0][0]</code>
<code>dense_3 (Dense)</code>	<code>(None, 2)</code>	202	<code>dense_2[0][0]</code>
<hr/>			
Total params: 33,643,414			
Trainable params: 10,055,702			
Non-trainable params: 23,587,712			

Figure 5.10: Model Summary of ResNet50

### 5.3.5 DenseNet121

Dense Convolutional Network which is DenseNet is an architecture that spotlights on making the profound learning networks go considerably more profound, and yet making them more proficient to prepare, by utilizing more limited associations between the layers [33]. DenseNet is very much like ResNet for certain key distinctions. For instance, ResNet utilizes an added substance strategy that combines the preceding layer with the future layer, while DenseNet links the result of the preceding layer with the future layer. This is done to empower the greatest data stream between the layers of the organization.

Here, we used the Keras implementation of the DenseNet121 model . We used the weights learned from the ImageNet dataset. We didn’t use the 3 fully connected layers at the top of the network. Input shape of the images is 224 x 224 and there are 3 channels. We performed the 2D Global Average Pooling. Then we performed batch normalization. We used a dropout rate of 0.5. We used the “ReLU” activation function for the layers and again performed batch normalization and used a dropout rate of 0.5. For predictions, we used the “Softmax” activation function.

## 5.4 Fine Tuning

Fine-tuning is the process of fine-tuning or changing a model that has already been trained for one task to make it execute a second related task. A deep learning network that recognizes cars, for example, maybe fine-tuned to recognize trucks

batch_normalization (BatchNorm)	(None, 1024)	4096	global_average_pooling2d[0][0]
dropout (Dropout)	(None, 1024)	0	batch_normalization[0][0]
dense (Dense)	(None, 1024)	1049600	dropout[0][0]
dense_1 (Dense)	(None, 512)	524800	dense[0][0]
batch_normalization_1 (BatchNorm)	(None, 512)	2048	dense_1[0][0]
dropout_1 (Dropout)	(None, 512)	0	batch_normalization_1[0][0]
dense_2 (Dense)	(None, 2)	1026	dropout_1[0][0]
<hr/>			
Total params: 8,619,674			
Trainable params: 1,578,498			
Non-trainable params: 7,040,576			

Figure 5.11: Model Summary of DenseNet121

[25]. As proposed, we will be using Fine-tuning approach to detect Glaucoma from our dataset which will help to detect our wanted result in this study

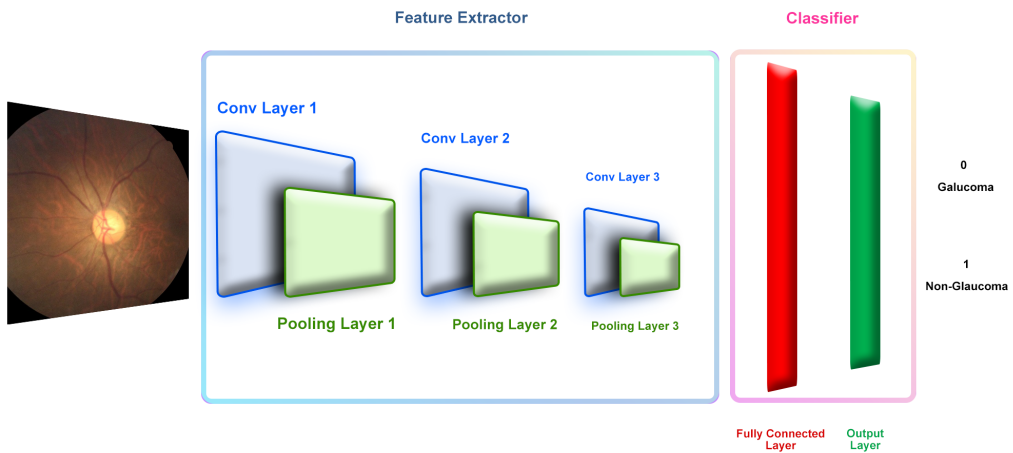


Figure 5.12: Fine-tuning by keeping the feature extractor's final layers trainable

### 5.4.1 Segments of CNN

The architecture of Convolutional Neural Networks is basically 3 types of layers.

- Convolutional
- Pooling
- Fully Connected

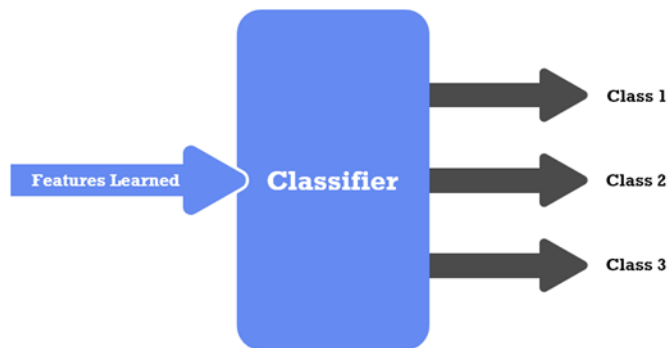


Figure 5.13: CNN Classifier

And basically, all these layers do these operations as bellow:

- Convolution operation
- Pooling operation
- Flattening
- Non-linear activation functions imply
- Optimization operation

### 5.4.2 Convolutional Operation

The convolutional layers, which are the fundamental building blocks of CNN, are responsible for convolution operations and produce feature maps that learn the features of the image taken as input by convolving appropriately learned filters or kernels with the input array or tensor, as shown in **figure 5.14**. A convolution layer, as shown in **figure 5.15**, has a number of feature maps that record new features and respond to feature hierarchy throughout the neural network, from the early layers to the distant edging layers.[29][34][30]

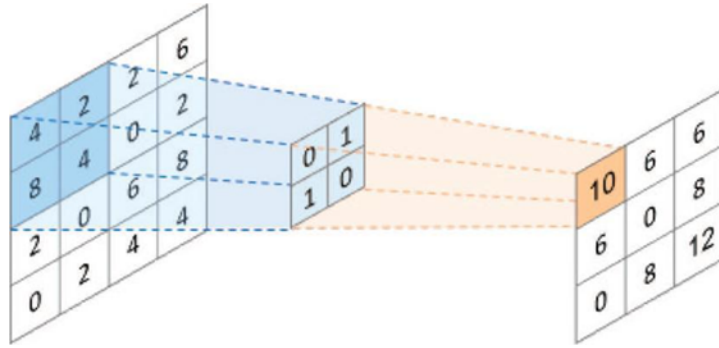


Figure 5.14: On the input tensor, a kernel is applied, resulting in a feature map

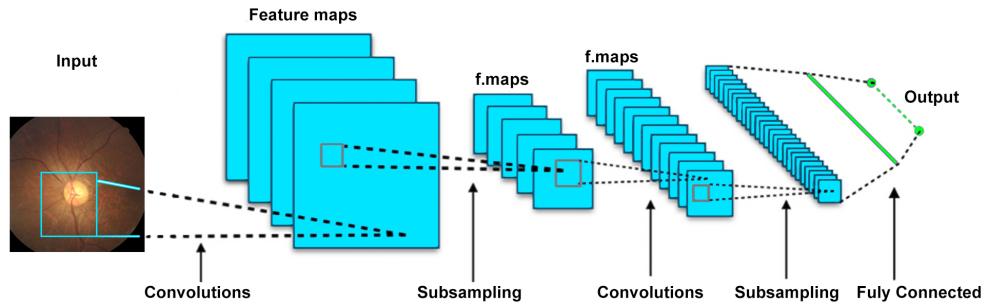


Figure 5.15: Planes shown are a feature map

### 5.4.3 Pooling Operation

The feature maps are pooled in order to extract more features and minimize their dimension[30]. In general, the pooling operation is carried out as follows:

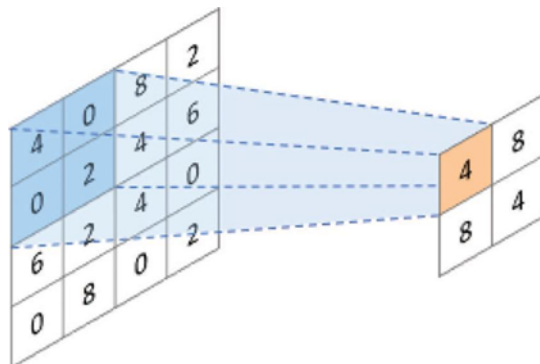


Figure 5.16: Pooling Operation

- **Max Pooling:** The maximum value of a patch of numbers from the feature map used as input is returned as an output. [30]

- **Average Pooling:** It produces the average value of a patch of numbers from the feature map that was used as input as an output. [34]
- **GlobalAveragePooling2D:** GlobalAveragePooling2D does something different. It applies average pooling on the spatial dimensions until each spatial dimension is one.

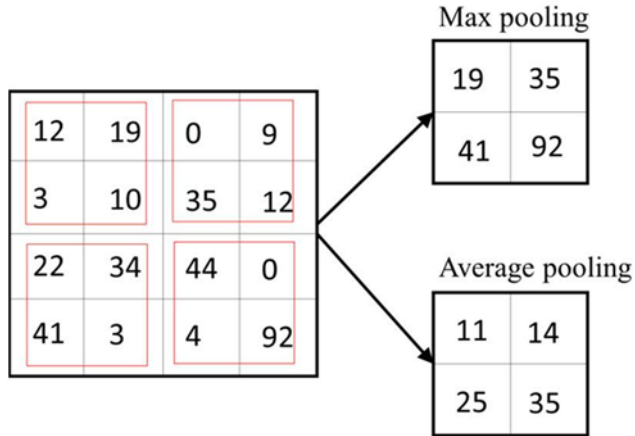


Figure 5.17: Max and Average Pooling

#### 5.4.4 Flattening Layers

Flattening is the process of turning data into a one-dimensional array for use in the following layer. To produce a single lengthy feature vector, we flatten the output of the convolutional layers. It's also linked to the final classification model, which is referred to as a fully-connected layer. [35]

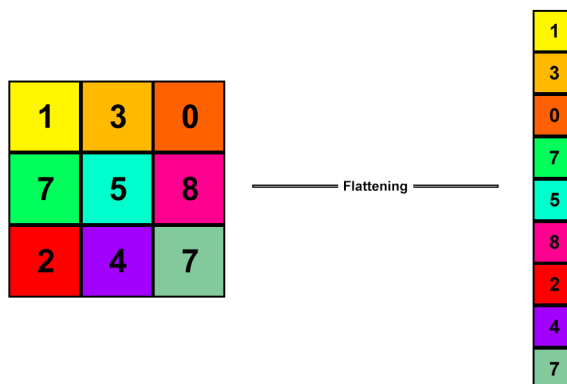


Figure 5.18: Pooling Matrix to Flattening.

### 5.4.5 Fully Connected Layers

In a neural network, fully connected layers are those where all of the inputs from one layer are connected to every activation unit of the subsequent layer. The last few layers in most standard machine learning models are fully connected layers that assemble the data collected by subsequent layers to produce the final output.[36]

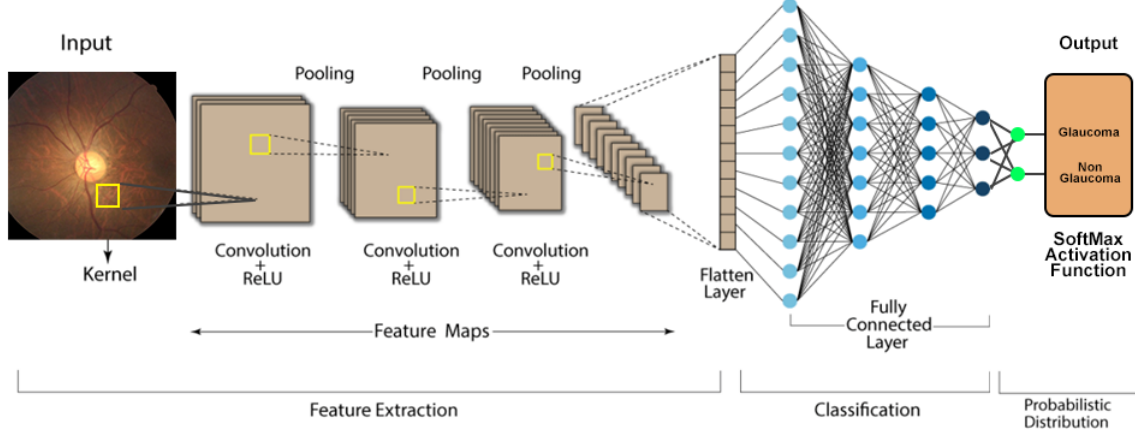


Figure 5.19: Fully Connected CNN classifying between classes

Fully connected layers or in other words dense layers take nonlinear activation functions, however, the final output layer of the fully connected layers take Softmax activation.

We are also going to use sigmoid and ReLU in both VGG-16 and InceptionV3.

### 5.4.6 Batch Normalization

While feeding input to Neural Networks, we do Batch Normalization because it makes the training faster and handles internal covariate shift. Again Normalizing the input for a similar range of values can speed up the learning. Because Batch Normalization normalizes the outputs of the activation functions in every layer of the neural network, not just in the inputs. In their original paper, Sergey et al. [37] claim that Batch Normalization reduces the internal covariate shift of the network.

### 5.4.7 Dropout

Adulteration of training information misleadingly regulates to overfit through dropout and other characteristical noise systems. Dropout holds out a kind of versatile regularization for summed up straight models [38]. Moreover, Dropout is a normal stochastic choice strategy in view of the neural organization [39]. This has the effect

of making the layer look and be treated as a layer with a particular measure of hubs and availability to the past layer. Essentially, a particular perspective on the designed layer is directed with each update to a layer during preparing.

## 5.5 Analysis

We have used VGG-16, VGG-19, DenseNet121, InceptionV3 and ResNet50 models for our study. Every model was compiled with Adam optimizer with the learning rate of 1e-5 in 50 epochs.

These are the score(validation accuracy) our models -

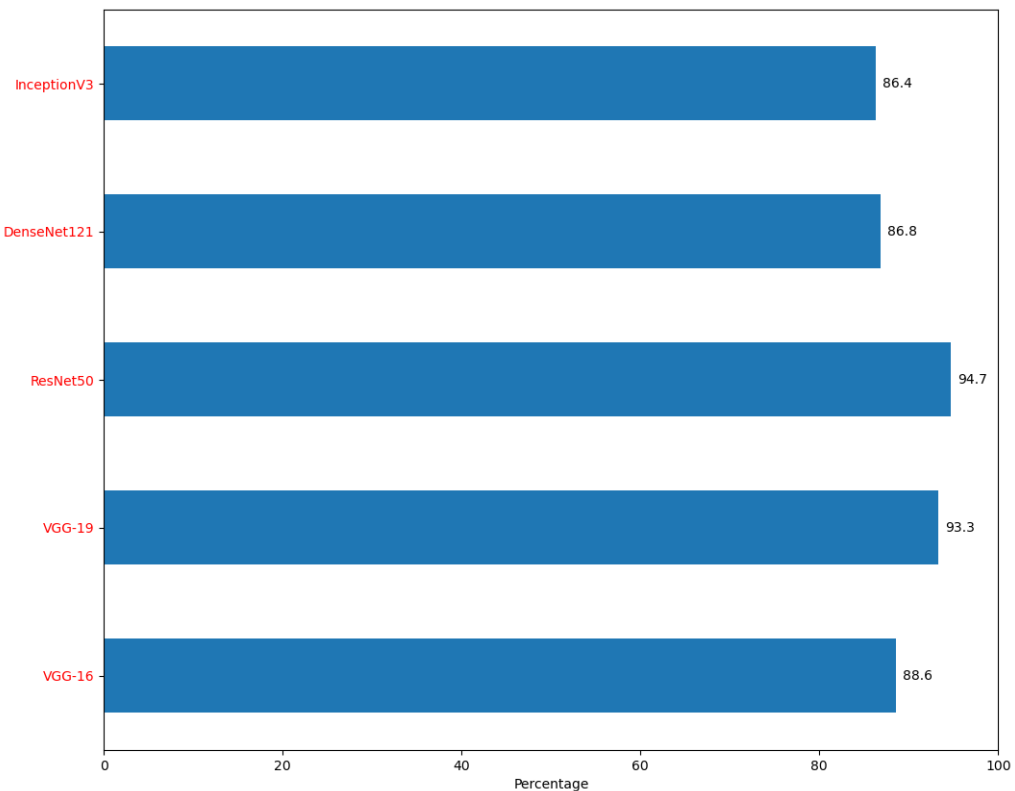


Figure 5.20: Fully Connected CNN classifying between classes

After 50 epochs, RestNet50 got the highest score among the other models with a validation accuracy of 94.7%.

These are the Train and Test accuracy and loss graph for each model.

Model Accuracy and Loss of VGG-16 -

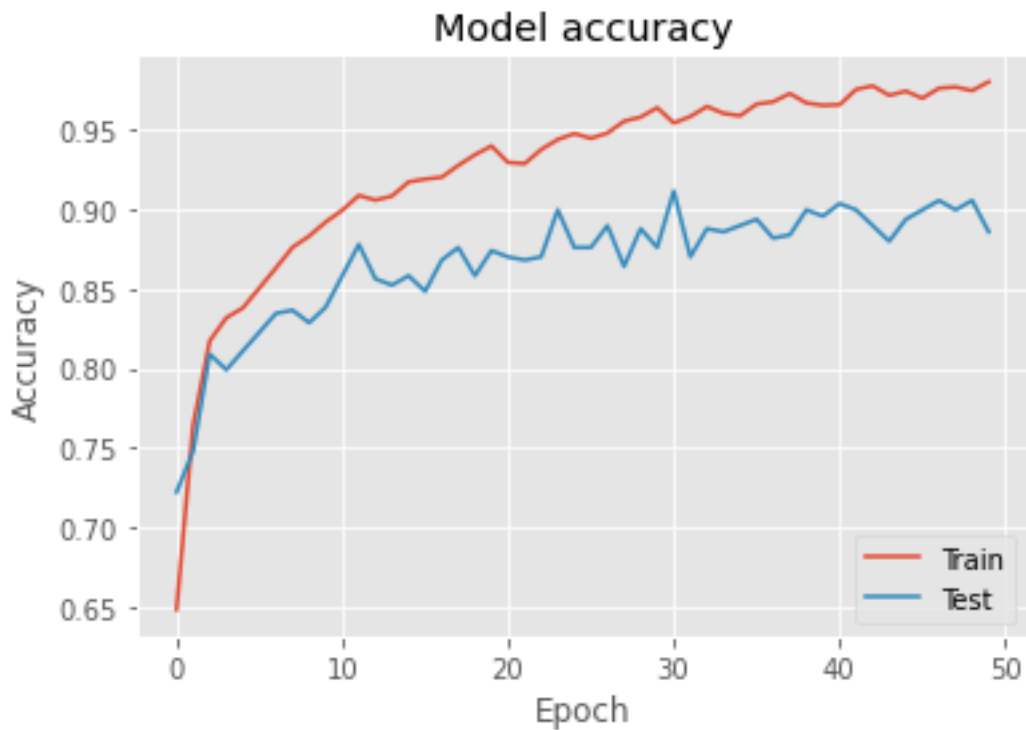


Figure 5.21: VGG-16 Model Train and Test Accuracy

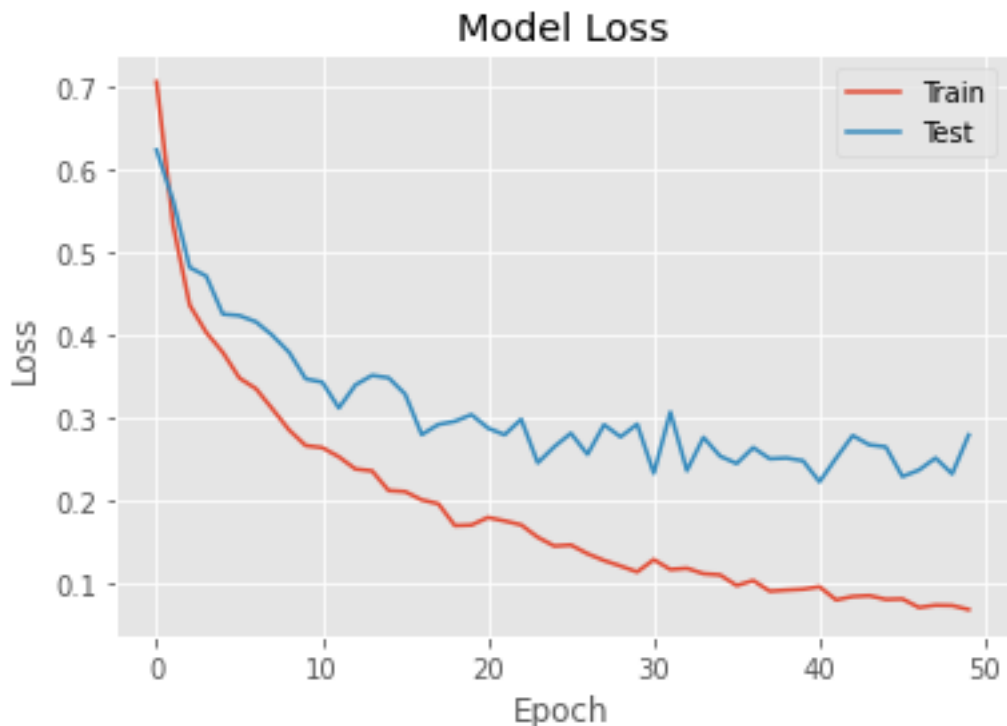


Figure 5.22: VGG-16 Model Train and Test Loss

Model Accuracy and Loss of VGG-19 -

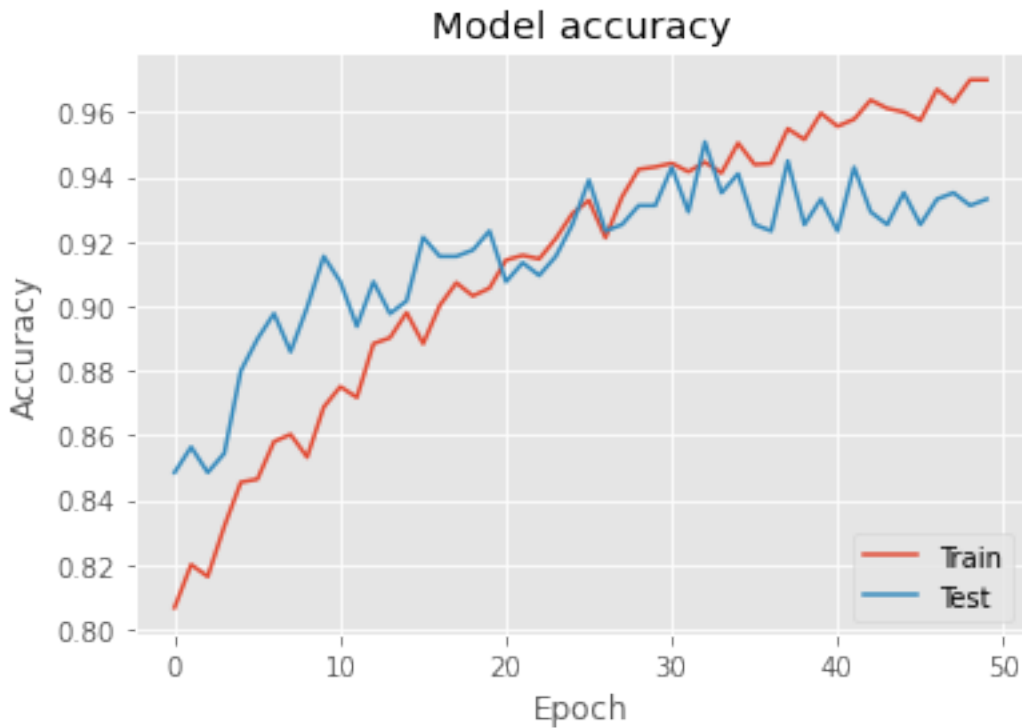


Figure 5.23: VGG-19 Model Train and Test Accuracy

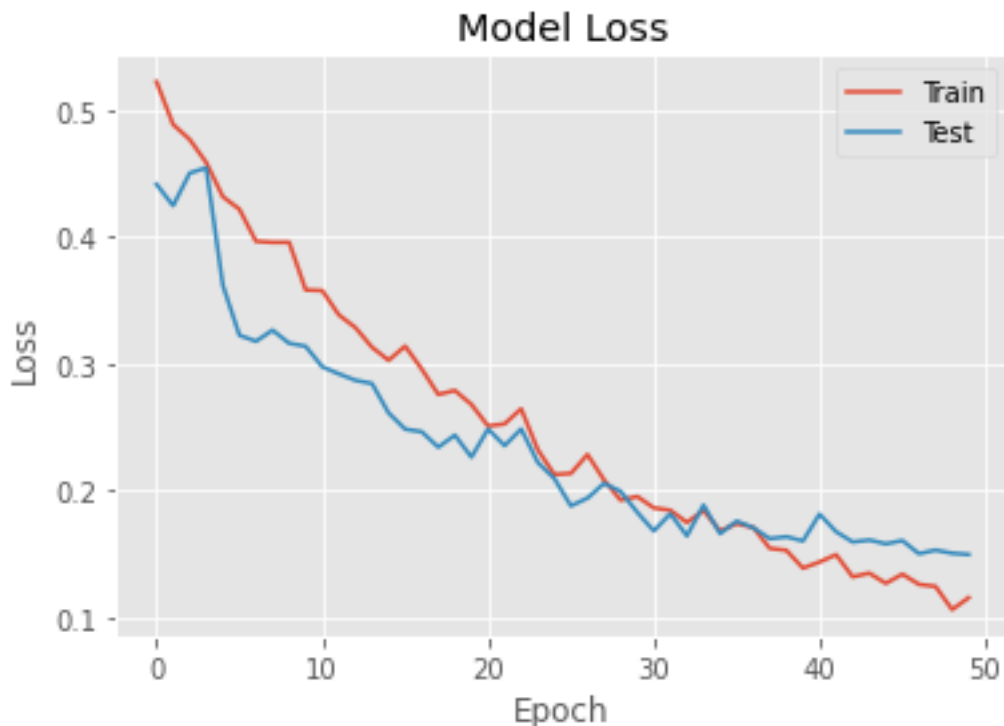


Figure 5.24: VGG-19 Model Train and Test Loss

Model Accuracy and Loss of ResNet50 -

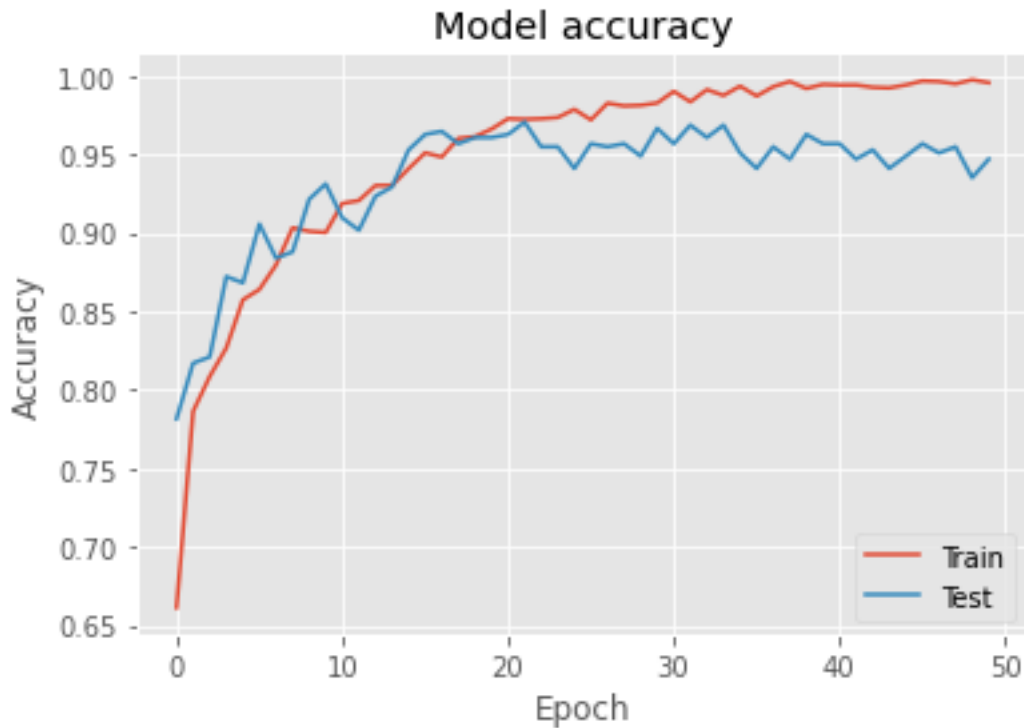


Figure 5.25: ResNet50 Model Train and Test Accuracy

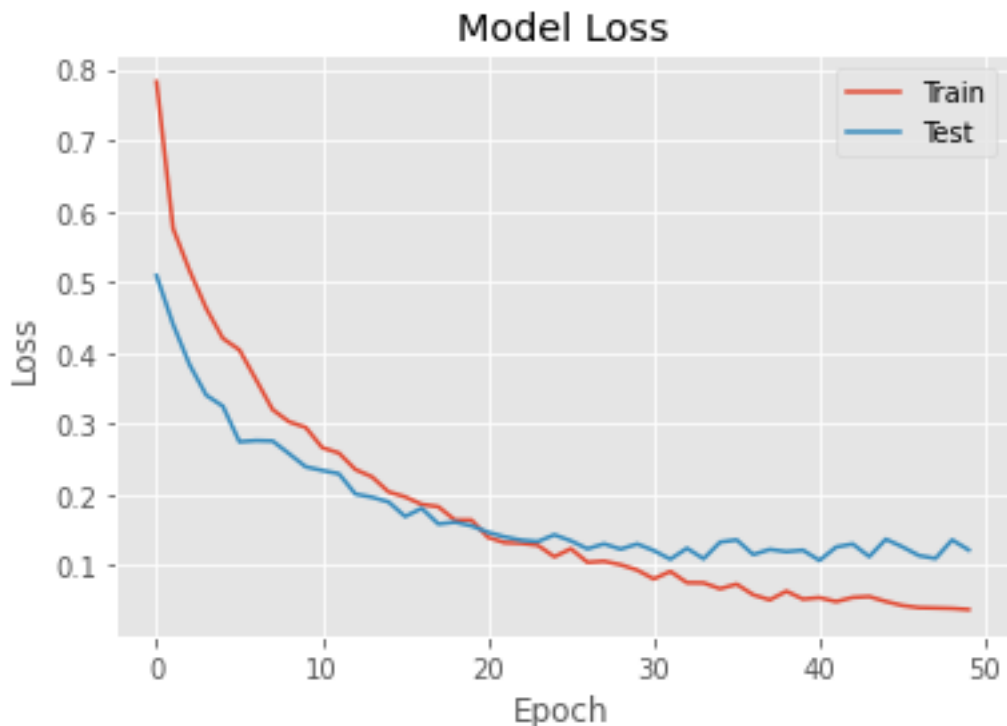


Figure 5.26: ResNet50 Model Train and Test Loss

Model Accuracy and Loss of DenseNet121 -

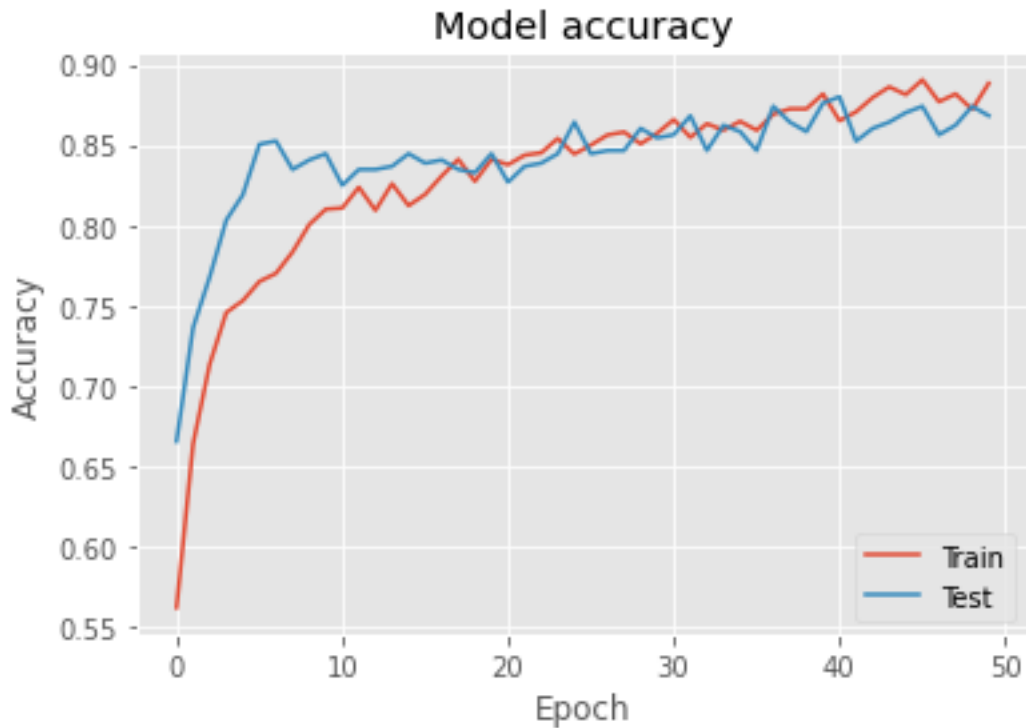


Figure 5.27: DenseNet121 Model Train and Test Accuracy

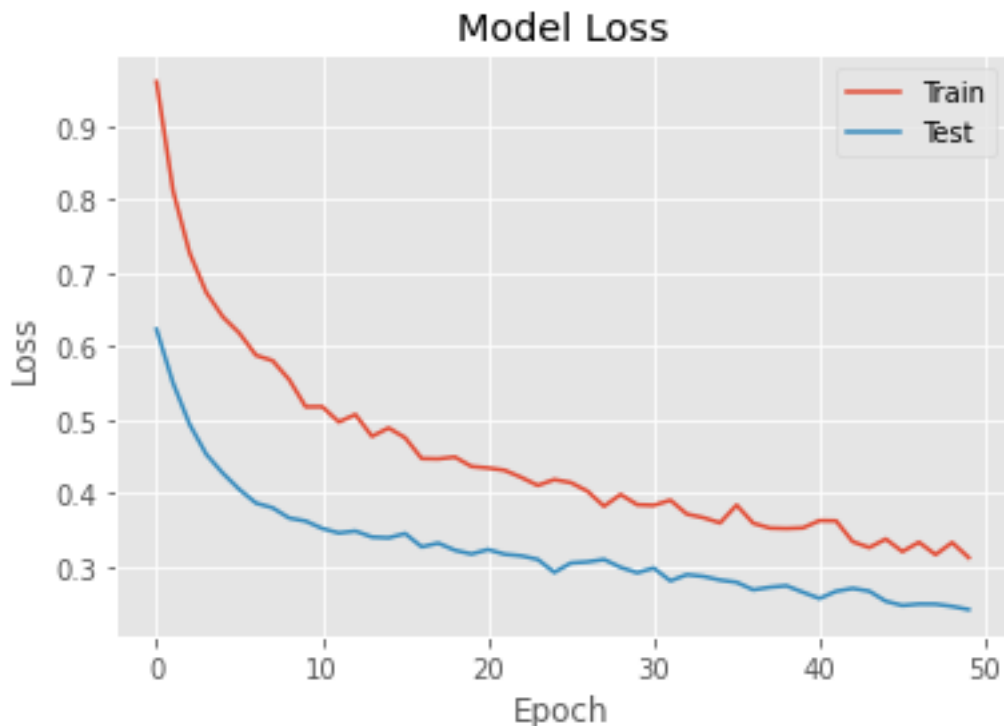


Figure 5.28: DenseNet121 Model Train and Test Loss

Model Accuracy and Loss of InceptionV3 -

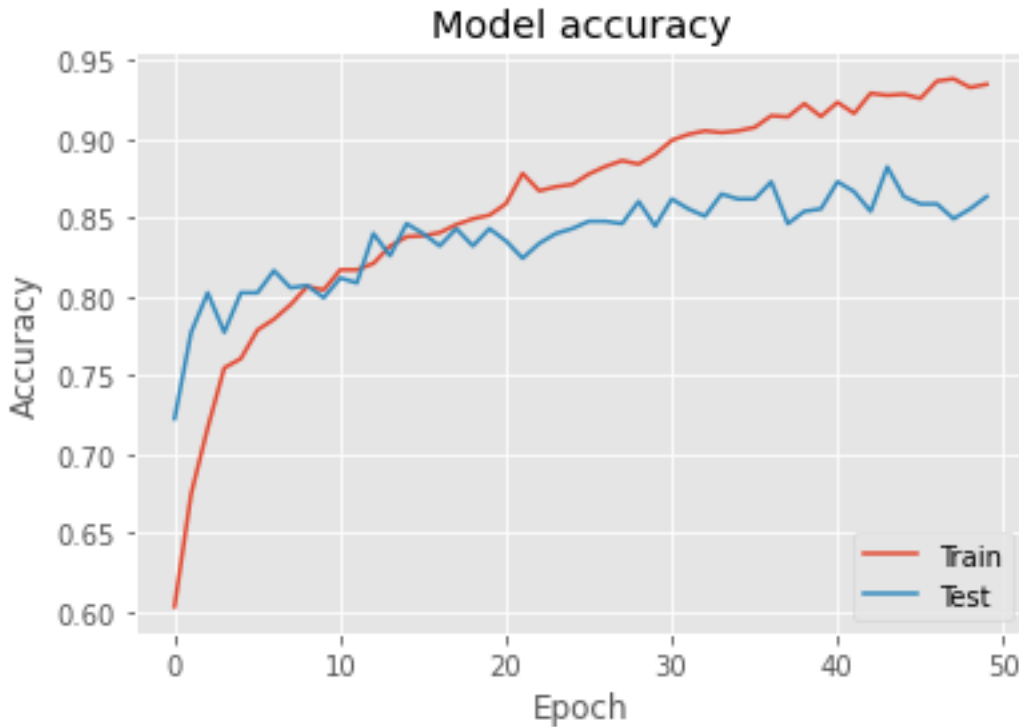


Figure 5.29: InceptionV3 Model Train and Test Accuracy

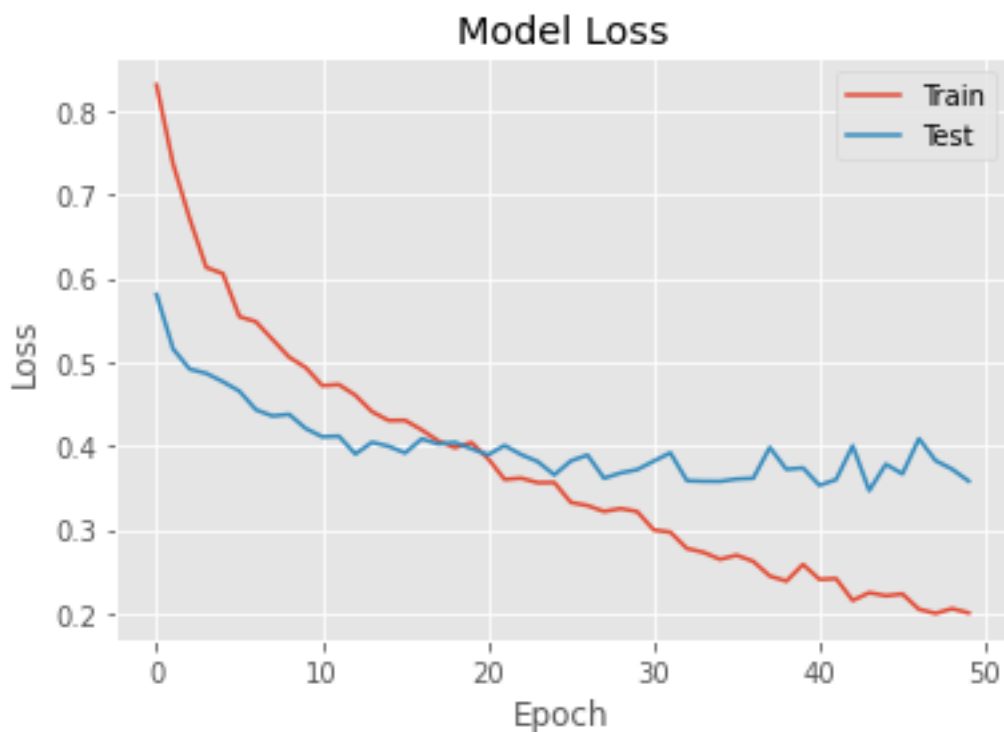


Figure 5.30: InceptionV3 Model Train and Test Loss

The shape and dynamics of a learning curve can be used to diagnose the behavior of a machine learning model and in turn perhaps suggest the type of configuration changes that may be made to improve learning and/or performance.

There are three common dynamics that you are likely to observe in learning curves. And they are:

- Underfit
- Overfit
- Good Fit

We know that smaller relative scores on the y-axis indicate more or better learning.

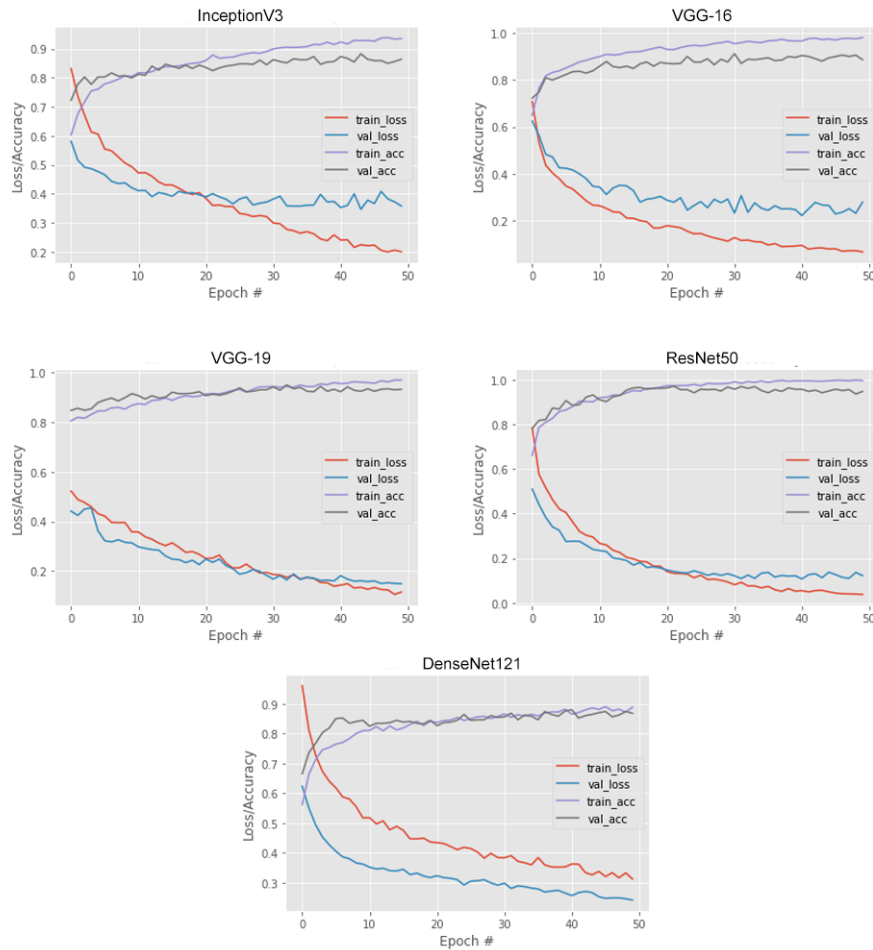


Figure 5.31: All Model's Train Test Accuracy and Loss Curve

Comparing All models' Accuracy and Loss graph together, we can see that VGG-19 and ResNet50 were the Good-Fit than the other models.

These are the Train sets, True and Predicted scores of classified and misclassified glaucoma and non-glaucoma results for each model based on the model's train

datasets prediction labels and the actual train labels. We have added a threshold of 0.5 for this train predicted visualization.

(the percentages are meaning the predicted train accuracy for the predicted labels calculated with the actual train labels)

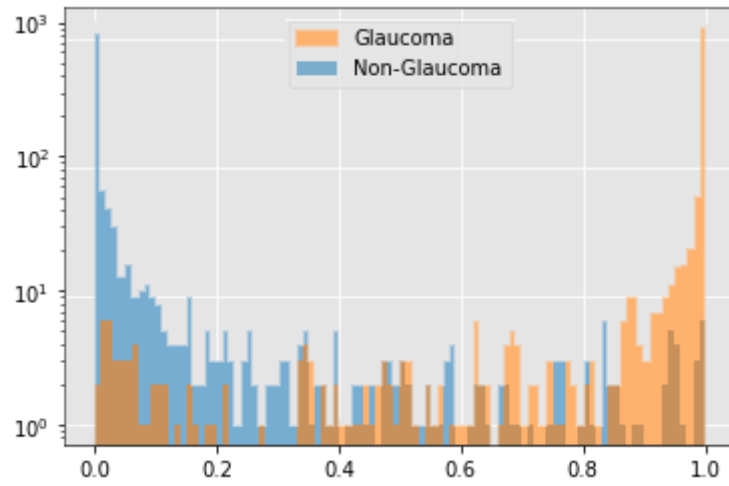


Figure 5.32: True and Predicted Train scores of DenseNet121

All 151 misclassified samples (93.83%)  
Glaucoma 74 misclassified samples (93.95%)  
Non-Glaucoma 77 misclassified samples (93.71%)

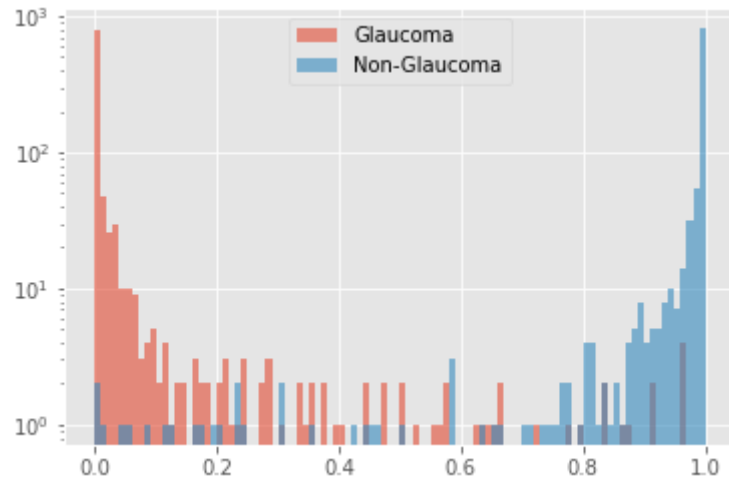


Figure 5.33: True and Predicted Train scores of InceptionV3

All 48 misclassified samples (97.65%)  
Glaucoma 22 misclassified samples (97.84%)  
Non-Glaucoma 26 misclassified samples (97.45%)

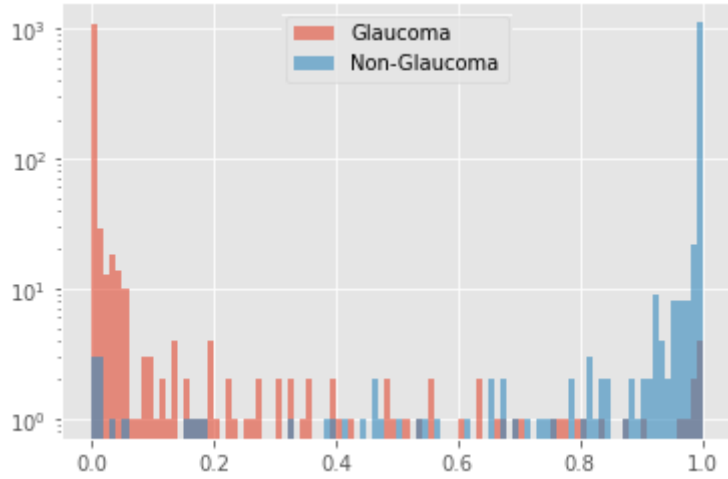


Figure 5.34: True and Predicted Train scores of VGG-16

All 47 misclassified samples (98.08%)  
Glaucoma 20 misclassified samples (98.37%)  
Non-Glaucoma 27 misclassified samples (97.79%)

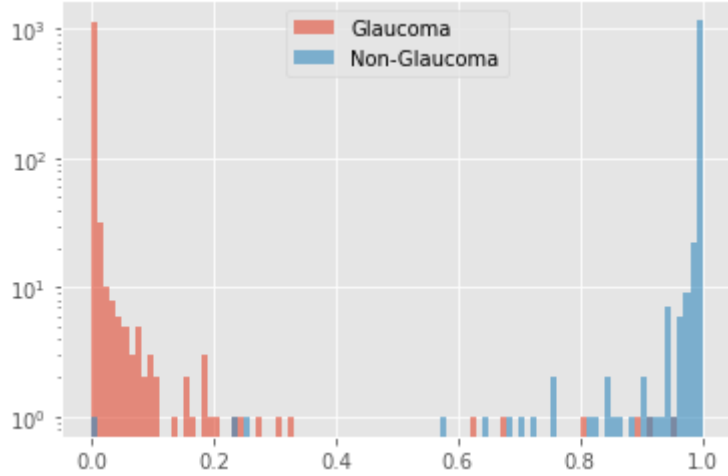


Figure 5.35: True and Predicted Train scores of VGG-19

All 17 misclassified samples (99.31%)  
Glaucoma 14 misclassified samples (98.86%)  
Non-Glaucoma 3 misclassified samples (99.75%)

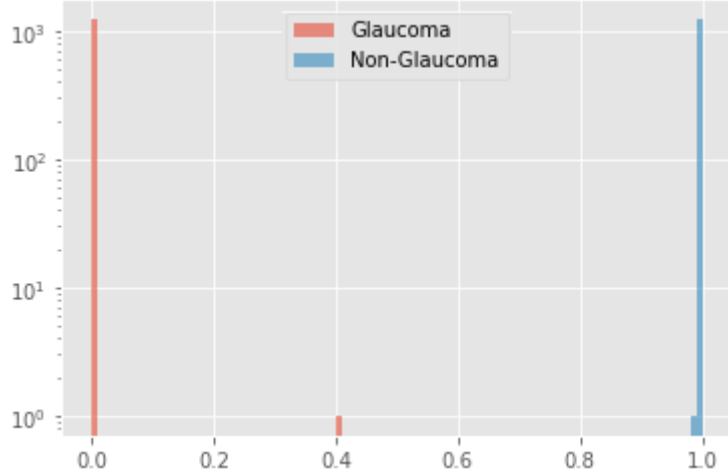


Figure 5.36: True and Predicted Train scores of ResNet50

All 0 misclassified samples (100.00%)  
 Glaucoma 0 misclassified samples (100.00%)  
 Non-Glaucoma 0 misclassified samples (100.00%)

Now, We have called the same function that we have used for the above Train predicted labels again with the same threshold of 0.5. But for now we have used the validation datasets prediction labels. And the results were -  
*(the percentages are meaning the predicted test/validation accuracy for the predicted labels calculated with the actual test/validation labels)*  
*( Here, G = Glaucoma and n-G = Non-Glaucoma )*

Model	All misclassified	G misclassified	n-G misclassified
DenseNet121	9 (86.76%)	4 (88.24%)	5 (85.29%)
InceptionV3	24 (85.88%)	16 (81.18%)	8 (90.59%)
VGG-16	8 (88.24%)	7 (79.41%)	1 (97.06%)
VGG-19	4 (94.12%)	3 (91.18%)	1 (97.06%)
ResNet50	3 (95.59%)	1 (97.06%)	2 (94.12%)

Table 5.3: True and Predicted Test scores of all Model

Now we have taken a single predicted batch from each model's prediction with the 0.5 threshold and plotted the misclassified glaucoma and non-glaucoma images, which we will use in Lime (XAI framework) to explain later.  
*( Here, G = Glaucoma and n-G = Non-Glaucoma )*

Model	Batch	G misclassified	n-G misclassified
DenseNet121	2 (32 in each)	3	5
InceptionV3	2 (32 in each)	2	7
VGG-16	2 (32 in each)	2	3
VGG-19	2 (32 in each)	1	4
ResNet50	2 (32 in each)	0	3

Table 5.4: True and Predicted Test scores of all Model

These are some of the misclassified images for all models with and undoing the existing preprocessing. Basically the model's preprocessing for these images ruined their actual color and contrast. Which led the model to predict wrong. By undoing the existing preprocessing we can see that for DesneNet121 the images got a little reddish and for other models, It got bluish.

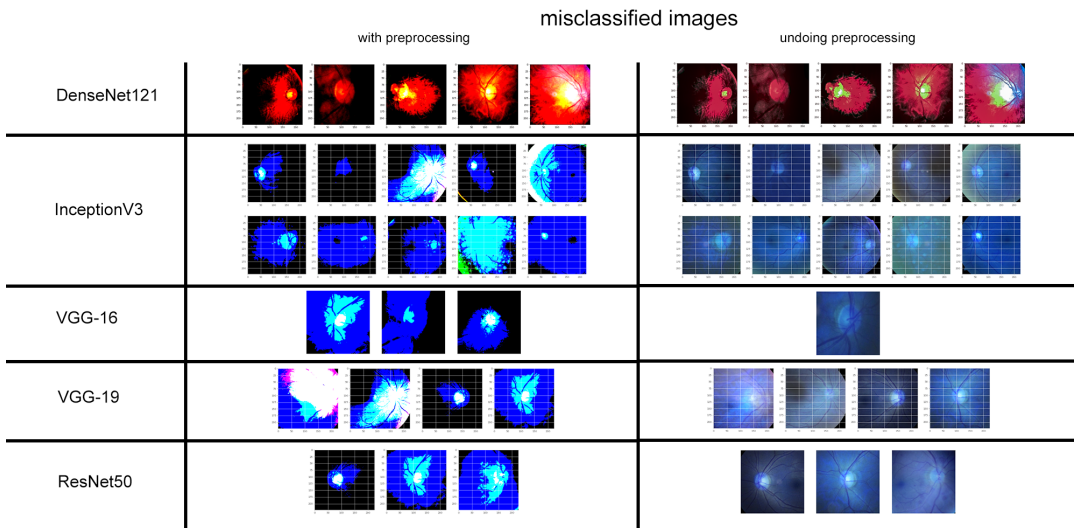


Figure 5.37: Misclassified images for all models with and without preprocessing

Now we will show the explanation for these preprocessed and misclassified images using an XAI[40] framework, **LIME**. Then we will apply Lime again on a single predicted raw fundus -image directly from the test dataset (labelled) directory to see the difference between a correctly predicted fundus image[42] and wrong predicted fundus image. Given below are the the misclassified image with preprocessing, Superpixels focused area and the model prediction explanation by Lime in DenseNet121

DenseNet121

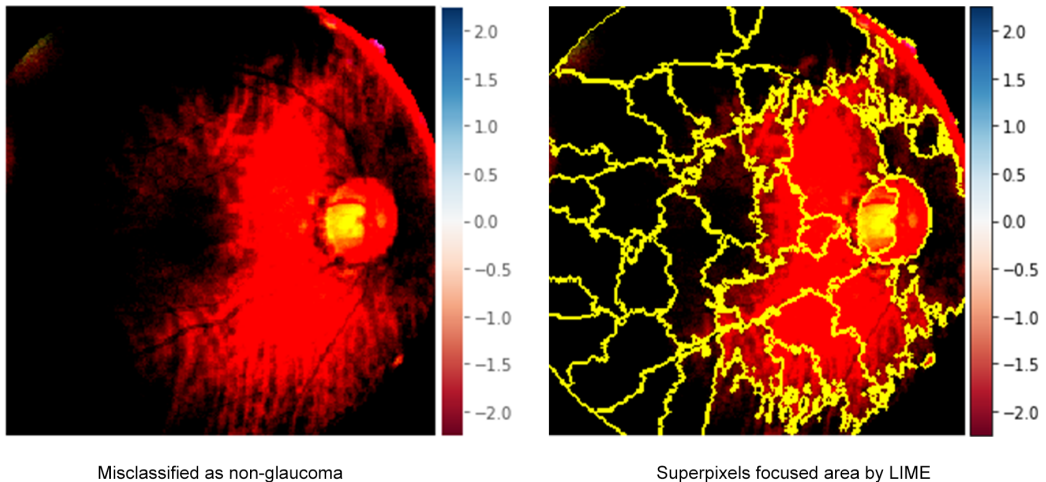


Figure 5.38: Misclassified image with preprocessing and Superpixels focused area by Lime in DenseNet121

DenseNet121

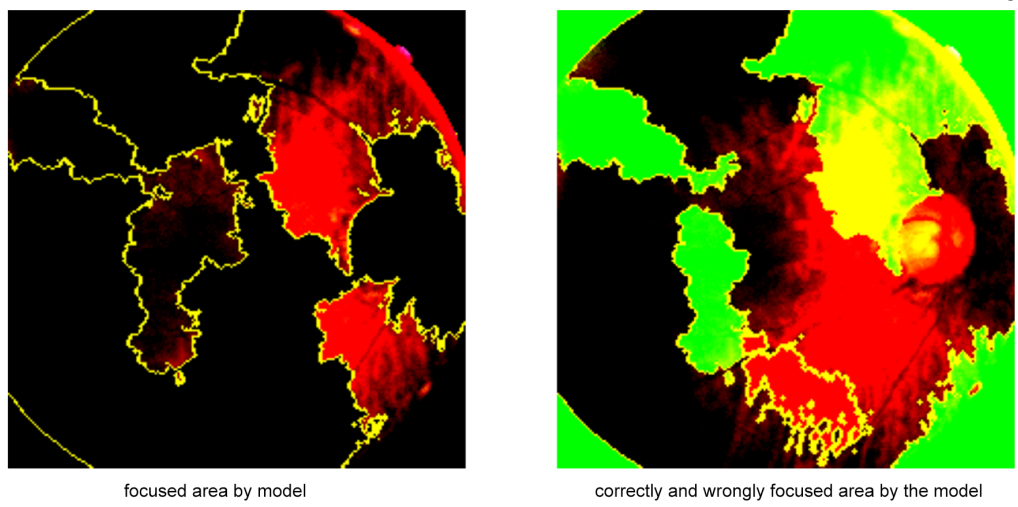


Figure 5.39: Lime Explanation for DenseNet121

Given below are the misclassified image with preprocessing, Superpixels focused area and the model prediction explanation by Lime in InceptionV3 -

InceptionV3

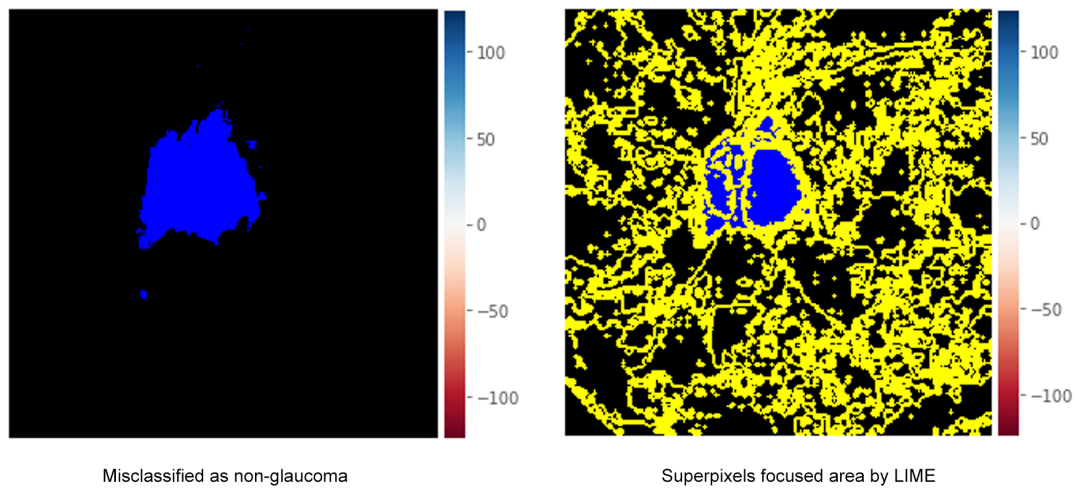


Figure 5.40: Misclassified image with preprocessing and Superpixels focused area by Lime in InceptionV3

InceptionV3

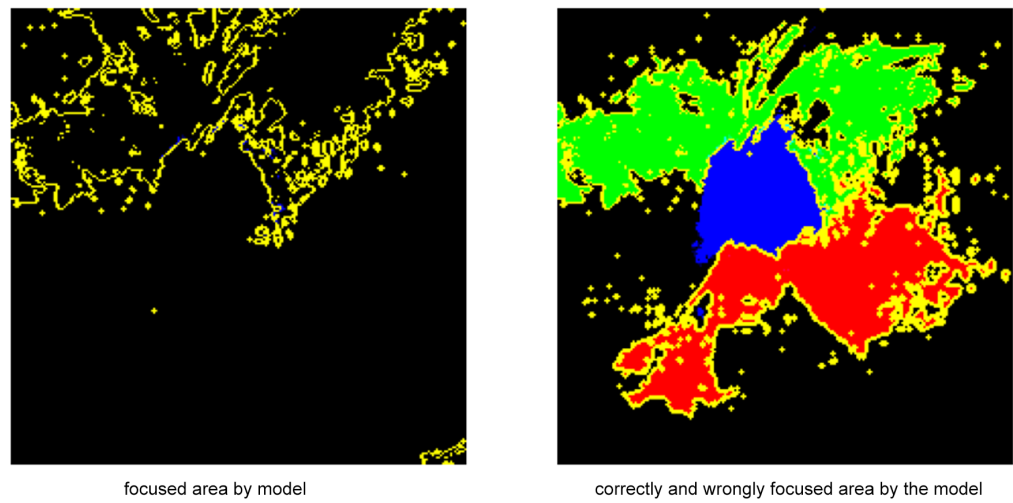


Figure 5.41: Lime Explanation for InceptionV3

Given below are the misclassified image with preprocessing, Superpixels focused area and the model prediction explanation by Lime in VGG-16 -

VGG-16

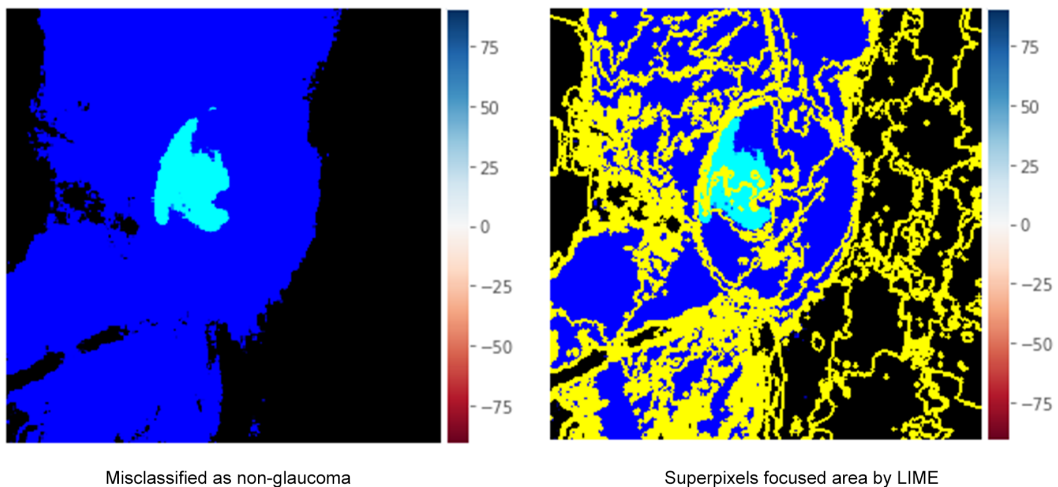


Figure 5.42: Misclassified image with preprocessing and Superpixels focused area by Lime in VGG-16

VGG-16

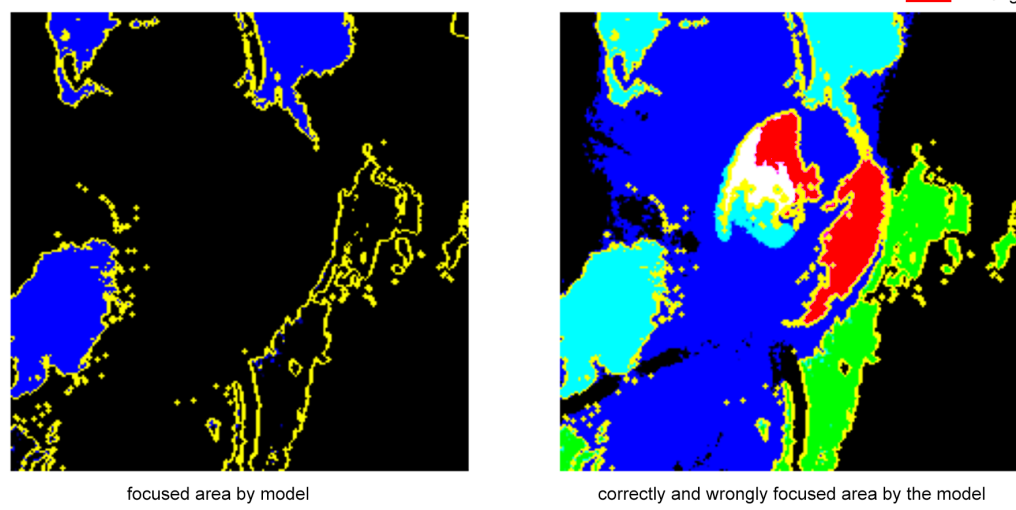


Figure 5.43: Lime Explanation for VGG-16

Given below are the the misclassified image with preprocessing, Superpixels focused area and the model prediction explanation by Lime in VGG-19 -

VGG-19

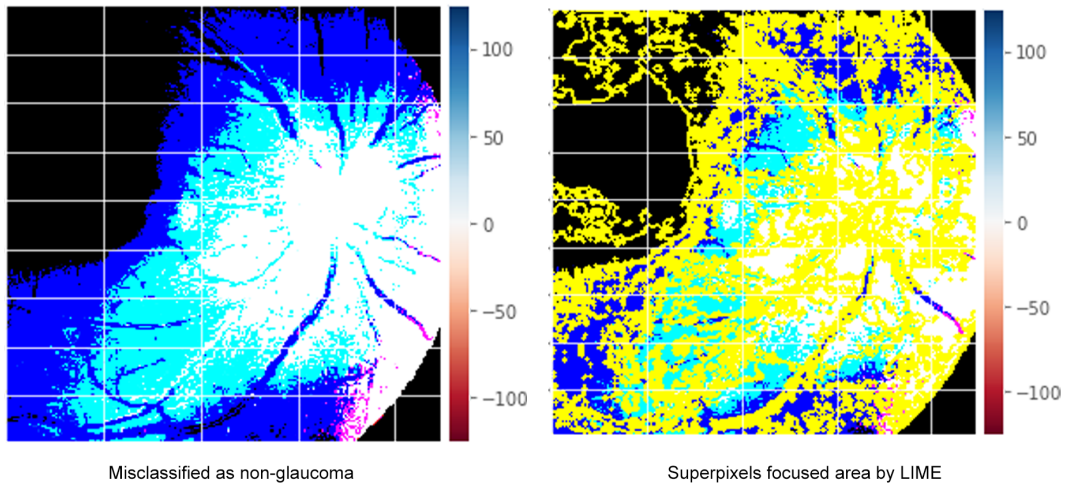


Figure 5.44: Misclassified image with preprocessing and Superpixels focused area by Lime in VGG-19

VGG-19

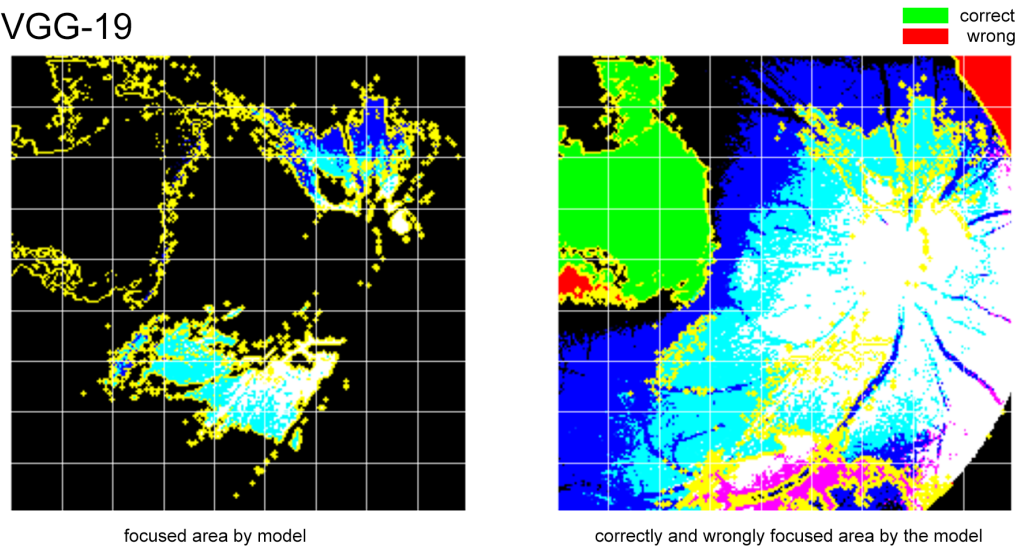


Figure 5.45: Lime Explanation for VGG-19

Given below are the misclassified image with preprocessing, Superpixels focused area and the model prediction explanation by Lime in ResNet50 -

ResNet50

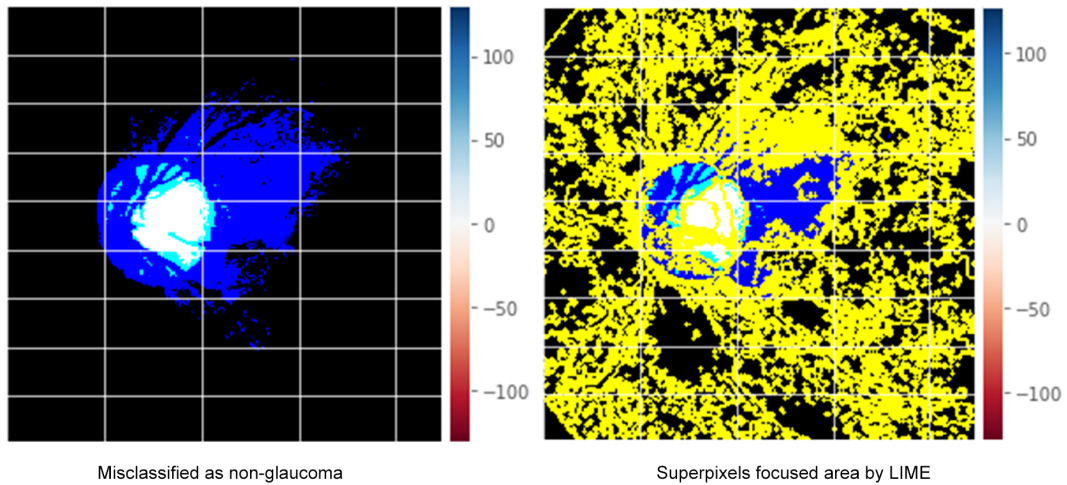


Figure 5.46: Misclassified image with preprocessing and Superpixels focused area by Lime in ResNet50

ResNet50

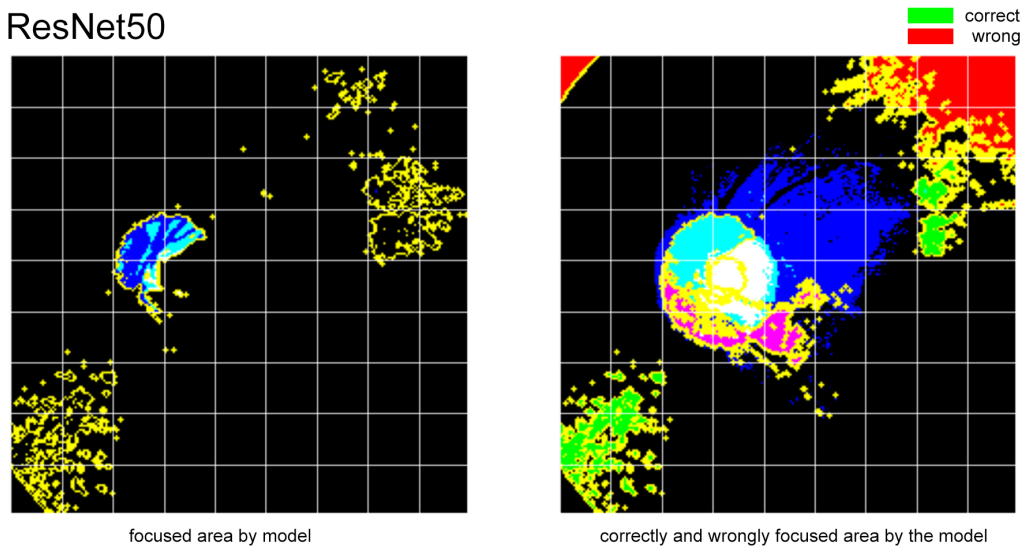


Figure 5.47: Lime Explanation for ResNet50

Now for the single predicted raw fundus image -

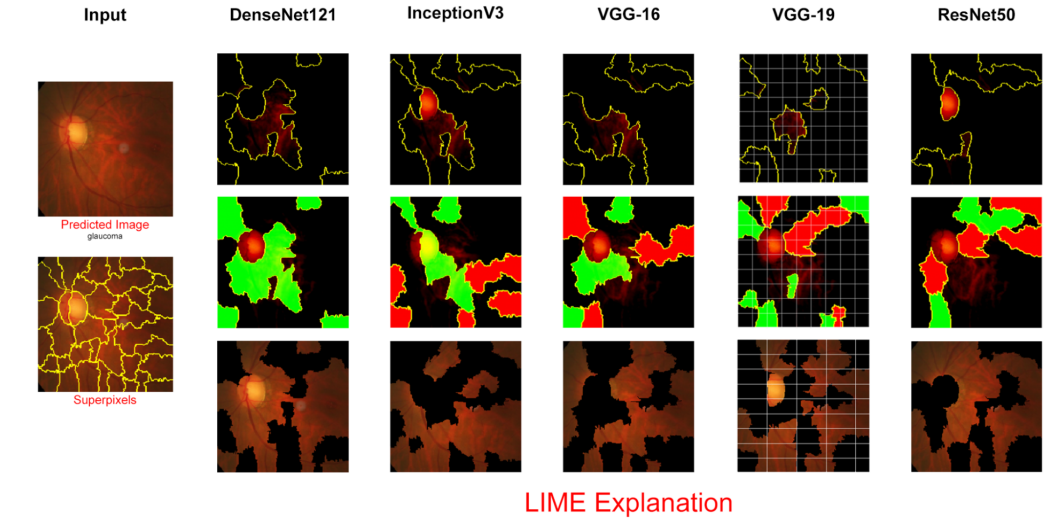


Figure 5.48: Lime Explanation for all models single image predictions

## 5.6 Result

These are the single image predictions of all models -  
*( here outputs are given in  $[n,m]$  format, where “m” means glaucoma score and “n” means non-glaucoma score )*

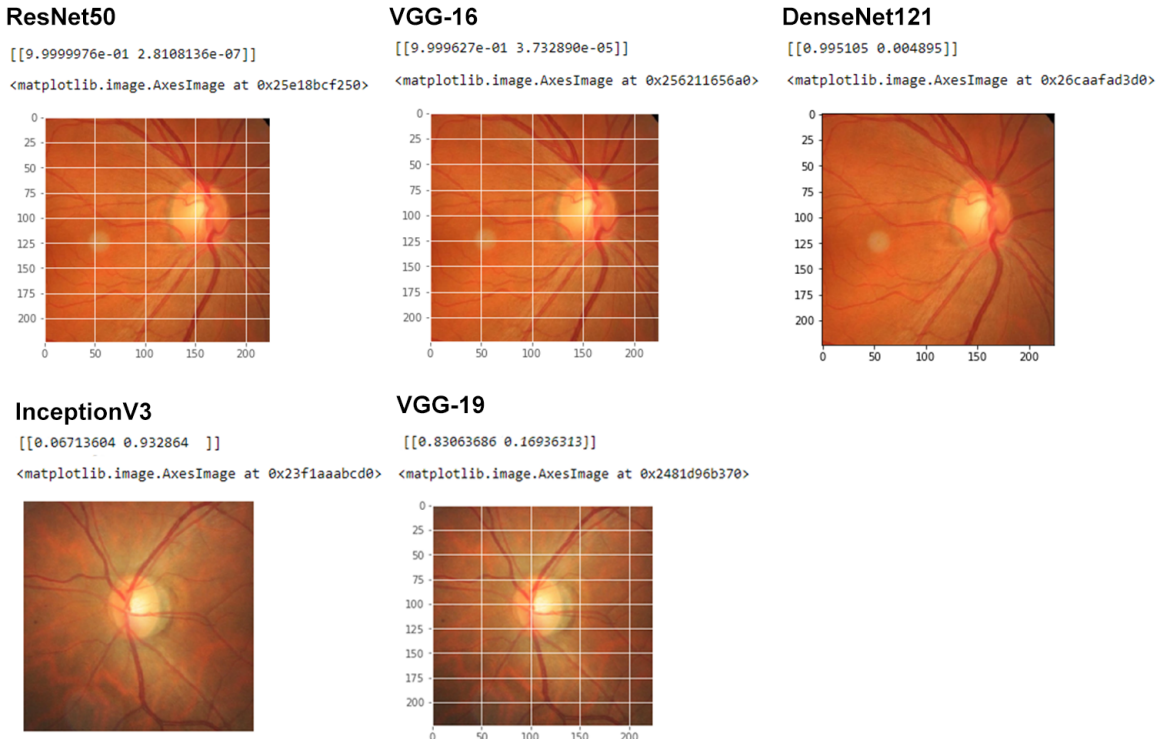


Figure 5.49: Single Image Predictions for all Model

These are batch (50 images/batch) image predictions of all models - ( here [1,0] means glaucoma and [0,1] means non-glaucoma )

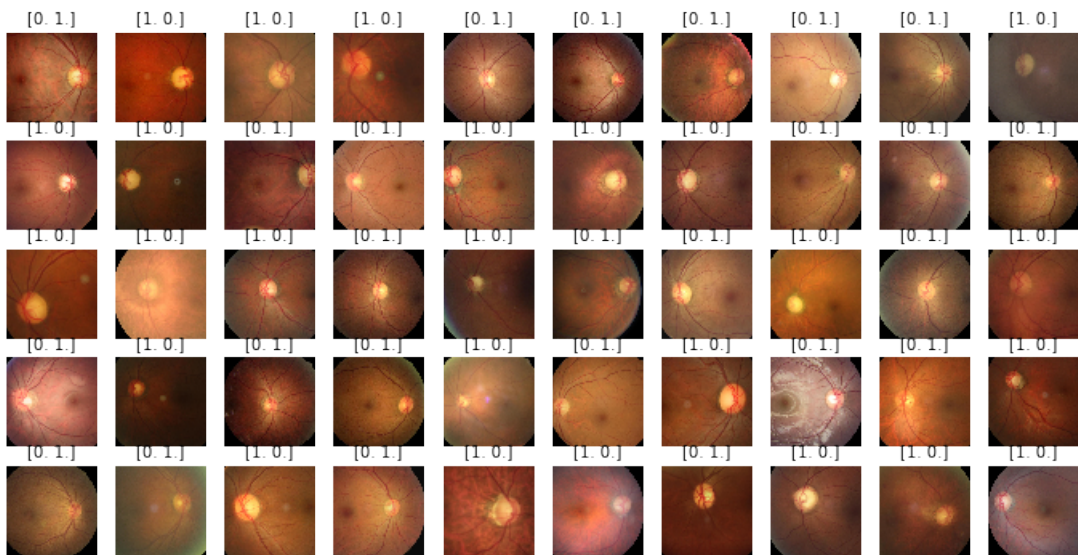


Figure 5.50: Batch Predictions for DenseNet121

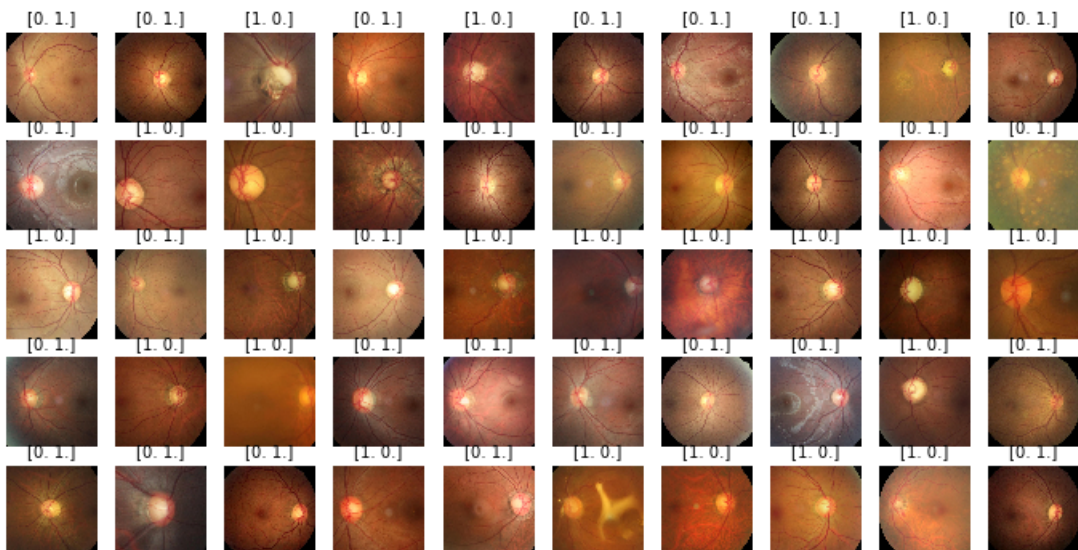


Figure 5.51: Batch Predictions for InceptionV3

These are batch (50 images/batch) image predictions of all models - ( here [1,0] means glaucoma and [0,1] means non-glaucoma )

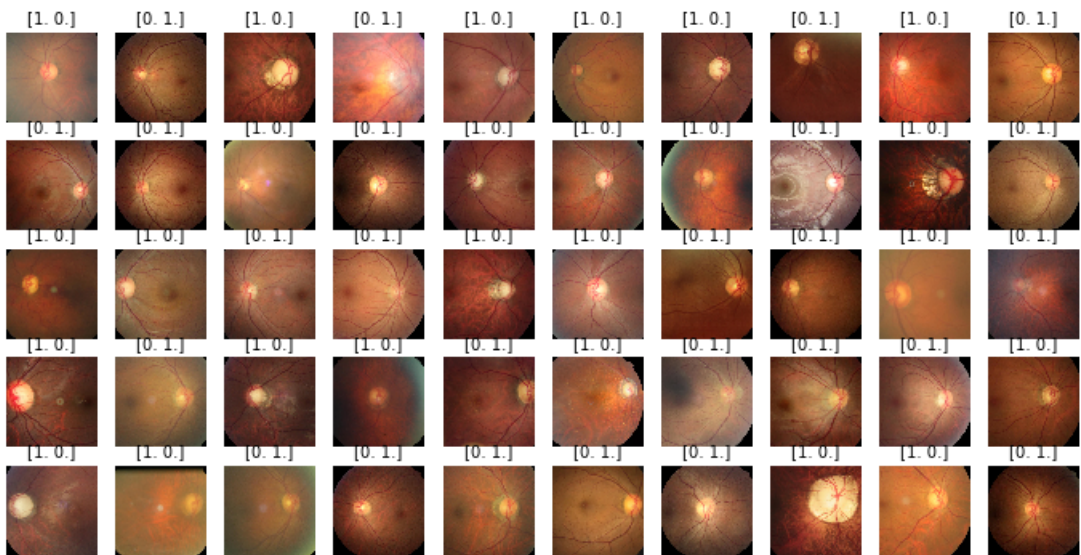


Figure 5.52: Batch Predictions for VGG-16

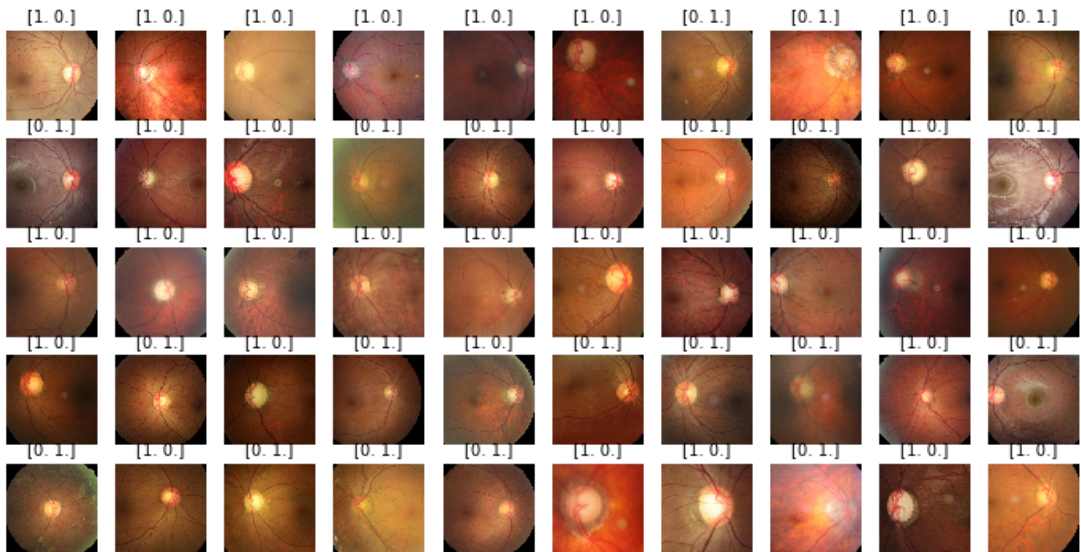


Figure 5.53: Batch Predictions for VGG-19

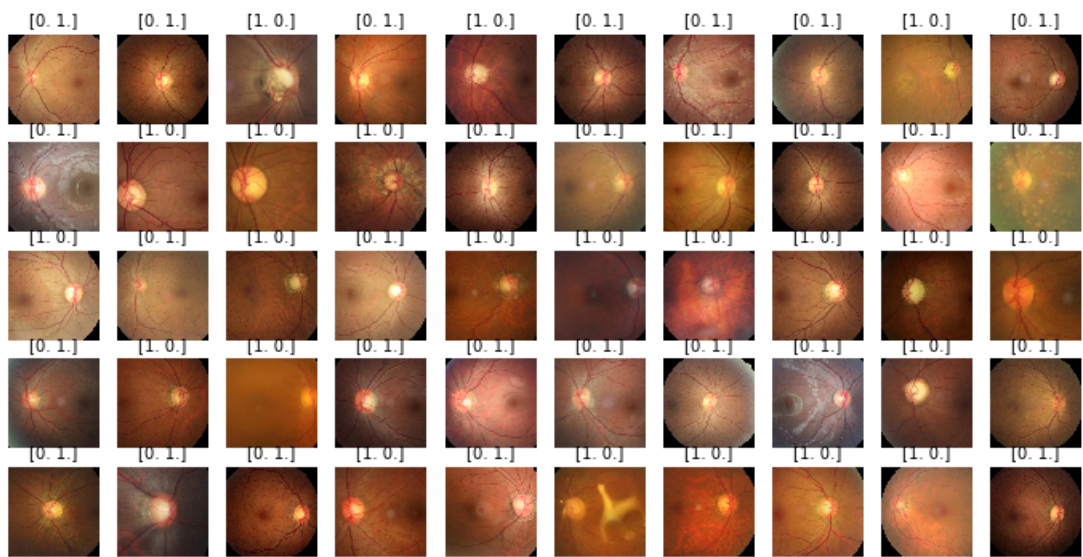


Figure 5.54: Batch Predictions for ResNet50

# **Chapter 6**

## **Conclusion**

### **6.1 Conclusion**

In this research, to attain the ultimate objective of our study in Glaucoma Diagnosis, the Black Box model was defined using Explainable Artificial Intelligence (XAI). As we have introduced our work we have done so far in this research paper. Through this research, we were led to more glaucoma diagnosis acceptability. Notably, glaucoma can take away the vision of a patient which is why it's more important to work for a better solution for early stage detection of glaucoma disease. For this reason, using the XAI, recognition, and treatment of Glaucoma can bring an immense change in the system which is very important, as reducing the number of blindness caused by glaucoma through early proper detection and treatment of the disease is going to be a huge success to celebrate. Because around the world 1 out of 15 people are blind because of it. Statistics show that even with the treatment 15our purpose we have used VGG-16, VGG-19, DenseNet121, InceptionV3 and ResNet50 models for our study. Every model was compiled with Adam optimizer with the learning rate of 1e-5 in 50 epochs. If we look at the score which is validation accuracy for our models we can see that in InceptionV3 we got 86.4% accuracy, in DenseNet121 we got 86.8% accuracy, in ResNet50 we got 94.7% accuracy, in VGG-19 we got 93.3% accuracy and lastly in VGG-16 we got 88.6% accuracy. As the results showed, after 50 epochs, RestNet50 got the highest score among the other models with a validation accuracy of 94.7%. Afterwards we compared all models' accuracy and loss graph together, where we can see that VGG-19 and ResNet50 were the Good-Fit than the other models. So for our purpose we are proposing to use the LIME for getting rid of the very lessened percentage in accuracy. Thereupon, in this research authors mentioned and showed how they have used Deep Neural Network Leveraging Explainable Artificial Intelligence to reduce the amount of Glaucoma Patients through early detection. Since there still is no known approach to prevent glaucoma, glaucoma-related blindness or major visual loss can be avoided if the condition is detected at an early stage. As now the AI has been improved and gained reliability in the medical sector so as per research it can be prevented by early detection. To sum up, we can say this research has achieved the goal to bring more accuracy, reliability and committed to improving more in Glaucoma diagnosis to make a difference in human life and contribute accordingly.

## Bibliography

- [1] Salam, A. A., Khalil, T., Akram, M. U., Jameel, A., Basit, I. (2016). Automated detection of glaucoma using structural and non structural features. SpringerPlus, 5(1).  
<https://doi.org/10.1186/s40064-016-3175-4>
- [2] Ran, A., Cheung, C. Y. (2021). Deep Learning-Based Optical Coherence Tomography and Optical Coherence Tomography Angiography Image Analysis: An Updated Summary. Asia-Pacific Journal of Ophthalmology, 10(3), 253–260.  
<https://doi.org/10.1097/apo.0000000000000405>
- [3] Aleci, C. (2020). Detection of Visual Field Loss Progression in Glaucoma: An Overview and Food for Thought. Ophthalmology Research: An International Journal, 16–24.  
<https://doi.org/10.9734/or/2020/v13i130158>
- [4] Saha, S., Wang, Z., Sadda, S., Kanagasingam, Y., Hu, Z. (2020). Visualizing and understanding inherent features in SD-OCT for the progression of age-related macular degeneration using deconvolutional neural networks. Applied AI Letters, 1(1).  
<https://doi.org/10.1002/ail2.16>
- [5] Civit-Masot, J., Dominguez-Morales, M. J., Vicente-Diaz, S., Civit, A. (2020). Dual Machine-Learning System to Aid Glaucoma Diagnosis Using Disc and Cup Feature Extraction. IEEE Access, 8, 127519–127529.  
<https://doi.org/10.1109/access.2020.3008539>
- [6] Diabetic Retinopathy — National Eye Institute. (2021, July 30). National Eye Institute.  
<https://www.nei.nih.gov/learn-about-eye-health/eye-conditions-and-diseases/diabetic-retinopathy>
- [7] Types of Glaucoma.(2020, June 2). Glaucoma Research Foundation.  
<https://www.glaucoma.org/glaucoma/types-of-glaucoma.php:%7E:text=There%20are%20several%20types%20of,or%20pressure%20inside%20the%20eye>
- [8] Saba, T., Khan, M. W., Yasmin, M., Sharif, M. (2017). CDR based glaucoma detection using fundus images: a review. International Journal of Applied Pattern Recognition, 4(3), 261.  
<https://doi.org/10.1504/ijapr.2017.10007613>
- [9] Thakoor, K. A., Li, X., Tsamis, E., Sajda, P., Hood, D. C. (2019). Enhancing the Accuracy of Glaucoma Detection from OCT Probability Maps using Convolutional Neural Networks. 2019 41st Annual International Conference of the IEEE Engineering in Medicine and Biology Society (EMBC).  
<https://doi.org/10.1109/embc.2019.8856899>

- [10] Lim, T. C., Chattopadhyay, S., Acharya, U. R. (2012). A survey and comparative study on the instruments for glaucoma detection. *Medical Engineering Physics*, 34(2), 129–139.  
<https://doi.org/10.1016/j.medengphy.2011.07.030>
- [11] Muddamsetty, S. M., Jahromi, M. N. S., Moeslund, T. B. (2021b). Expert Level Evaluations for Explainable AI (XAI) Methods in the Medical Domain. *Pattern Recognition. ICPR International Workshops and Challenges*, 35–46.  
[https://doi.org/10.1007/978-3-030-68796-0\\_3](https://doi.org/10.1007/978-3-030-68796-0_3)
- [12] Abbas, Q. (2017). Glaucoma-Deep: Detection of Glaucoma Eye Disease on Retinal Fundus Images using Deep Learning. *International Journal of Advanced Computer Science and Applications*, 8(6).  
<https://doi.org/10.14569/ijacsa.2017.080606>
- [13] Dervisevic, E., Pavljasevic, S., Dervisevic, A., Kasumovic, A. (2016). Challenges In Early Glaucoma Detection. *Medical Archives*, 70(3), 203.  
<https://doi.org/10.5455/medarh.2016.70.203-207>
- [14] R. Asaoka, H. Murata, A. Iwase, M. Araie, “Detecting preperimetric Glaucoma with Standard Automated Perimetry Using a Deep Learning Classifier,” *Ophthalmology*, vol. 123, pp. 1974–1980, September 2016.
- [15] Mayro, E.L., Wang, M., Elze, T. et al. The impact of artificial intelligence in the diagnosis and management of glaucoma. *Eye* 34, 1–11 (2020).  
<https://doi.org/10.1016/j.ophtha.2016.05.029>
- [16] Shabbir, A., Rasheed, A., Shehraz, H., Saleem, A., Zafar, B., Sajid, M., Ali, N., Dar, S. H., Shehryar, T. (2021). Detection of glaucoma using retinal fundus images: A comprehensive review. *Mathematical Biosciences and Engineering*, 18(3), 2033–2076.  
<https://doi.org/10.3934/mbe.2021106>
- [17] Brown, J. M., Leontidis, G. (2021). Deep learning for computer-aided diagnosis in ophthalmology: a review. *State of the Art in Neural Networks and their Applications*, 219–237.  
<https://www.sciencedirect.com/science/article/pii/B9780128197400000115>
- [18] Sau, P. C., Gupta, M., Kumar, D. (2021). A Comparative Study: Glaucoma Detection Using Deep Neural Networks. In *Proceedings of International Conference on Big Data, Machine Learning and their Applications* (pp. 85-97). Springer, Singapore.  
[https://link.springer.com/chapter/10.1007/978-981-15-8377-3\\_8](https://link.springer.com/chapter/10.1007/978-981-15-8377-3_8)
- [19] Greco, A., Rizzo, M. I., De Virgilio, A., Gallo, A., Fusconi, M., de Vincentiis, M. (2016). Emerging concepts in Glaucoma and review of the literature. *The American Journal of Medicine* (2016).  
<https://doi.org/10.1016/j.amjmed.2016.03.038>

- [20] Pascolini, D., Mariotti, S. P. (2012). Global estimates of visual impairment: 2010. *British Journal of Ophthalmology*, 96(5), 614-618.  
<https://bj.o.bmj.com/content/96/5/614.short>
- [21] Goldbaum MH, Sample PA, White H, Colt B, Raphaelian P, Fechtner RD, et al. Interpretation of automated perimetry for glaucoma by neural network. *Invest Ophthalmol Vis Sci*. 1994;35:3362–73.  
[https://www.researchgate.net/publication/15141759\\_Interpretation\\_of\\_automated\\_perimetry\\_for\\_glucoma\\_by\\_neural\\_network](https://www.researchgate.net/publication/15141759_Interpretation_of_automated_perimetry_for_glucoma_by_neural_network)
- [22] Murphy, A. M., Moore, C. M. M. (2020). Fully connected neural network.  
<https://radiopaedia.org/articles/fully-connected-neural-network>
- [23] Brownlee, J. (2020, August 14). What is Deep Learning? Machine Learning Mastery.  
<https://machinelearningmastery.com/what-is-deep-learning/>
- [24] Khan, S. M. K. (2021, January 3). Papers with Code - LAG Dataset. *The Lancet*.  
<https://paperswithcode.com/dataset/lag>
- [25] How to fine-tune your artificial intelligence algorithms  
<https://www.allerin.com/blog/how-to-fine-tune-your-artificial-intelligence-algorithms>
- [26] Saxena, A., Vyas, A., Parashar, L., Singh, U. (2020, July). A glaucoma detection using a convolutional neural network. In 2020 International Conference on Electronics and Sustainable Communication Systems (ICESC) (pp. 815-820). IEEE.  
<https://ieeexplore.ieee.org/abstract/document/9155930/>
- [27] Dervisevic, E., Pavljasevic, S., Dervisevic, A., Kasumovic, S. S. (2016). Challenges In Early Glaucoma Detection. *Medical archives (Sarajevo, Bosnia and Herzegovina)*, 70(3), 203–207.  
<https://doi.org/10.5455/medarh.2016.70.203-207>
- [28] Mash, Robert Becherer, Nicholas Woolley, Brian Pecarina, John. (2016). Toward aircraft recognition with convolutional neural networks.  
<https://doi.org/10.1109/NAECON.2016.7856803>.
- [29] Guo, T., Dong, J., Li, H., Gao, Y. (2017). Simple convolutional neural network on image classification. 2017 IEEE 2nd International Conference on Big Data Analysis (ICBDA).  
<https://doi.org/10.1109/icbda.2017.8078730>
- [30] Yamashita, R., Nishio, M., Do, R. K. G., Togashi, K. (2018). Convolutional neural networks: an overview and application in radiology. *Insights into Imaging*, 9(4), 611–629.  
<https://doi.org/10.1007/s13244-018-0639-9>

- [31] Yun-Cheng Tsai Predict Forex Trend via Convolutional Neural Networks  
<https://www.degruyter.com/document/doi/10.1515/jisys-2018-0074/html>
- [32] Kaushik, A. (2020, February 26). Understanding the VGG19 Architecture. OpenGenus IQ: Computing Expertise Legacy.  
<https://iq.opengenus.org/vgg19-architecture/#:%7E:text=VGG19%20is%20a%20variant%20of,VGG19%20has%2019.6%20billion%20FLOPs.>
- [33] Huang, G. (2016, August 25). Densely Connected Convolutional Networks. ArXiv.Org.  
<https://arxiv.org/abs/1608.06993>
- [34] S. Saha, A comprehensive guide to convolutional neural networks — the eli5 way, Available at  
<https://towardsdatascience.com/a-comprehensive-guide-to-convolutional-neural-networks-the-eli5-way-3bd2b1164a53>, 2018.
- [35] Jeong, J. (2021, December 7). The Most Intuitive and Easiest Guide for Convolutional Neural Network. Medium.  
<https://towardsdatascience.com/the-most-intuitive-and-easiest-guide-for-convolutional-neural-network-3607be47480>
- [36] Singh, S. P. (2019, March 2). Fully Connected Layer: The brute force layer of a Machine Learning model. OpenGenus IQ: Computing Expertise Legacy.  
<https://iq.opengenus.org/fully-connected-layer/>
- [37] Sergey Ioffe, Christian Szegedy.(2015). Batch Normalization: Accelerating Deep Network Training by Reducing Internal Covariate Shift.  
<https://arxiv.org/pdf/1502.03167.pdf>
- [38] S. Wager, S. Wang, and P. S. Liang, training as adaptive regularization”, in Advances in Neural Information Processing Systems 26, C. J. C. Burges, L. Bottou, M. Welling, Z. Ghahramani, and K. Q. Weinberger, Eds., Curran Associates, Inc., 2013, pp. 351-359. [Online].  
<http://papers.nips.cc/paper/4882-dropout-training-as-adaptive-regularization.pdf>.
- [39] Springenberg, J. T. (2014, December 21). Striving for Simplicity: The All Convolutional Net. ArXiv.Org. <https://arxiv.org/abs/1412.6806>
- [40] Dağlarlı, E. (2020). Explainable Artificial Intelligence (XAI) Approaches and Deep Meta-Learning Models. Advances and Applications in Deep Learning, 79.  
<https://www.intechopen.com/chapters/72398>
- [41] Shabbir, A., Rasheed, A., Shehraz, H., Saleem, A., Zafar, B., Sajid, M., ... Shehryar, T. (2021). Detection of glaucoma using retinal fundus images: A comprehensive review. Mathematical Biosciences and Engineering, 18(3), 2033-2076.  
<http://aimspress.com/article/doi/10.3934/mbe.2021106>

[42] Vejjanugraha, P., Kongprawechnon, W., Kondo, T., Tungpimolrut, K., Kotani, K. (2017). An automatic screening method for primary open-angle glaucoma assessment using binary and multi-class support vector machines. *ScienceAsia*, 43(4), 229.

<https://doi.org/10.2306/scienceasia1513-1874.2017.43.229>